Table 2. Cooperating genetic changes in leukemic mice belonging to groups 1 and 2

Group/tumor ID	Genotype	Stem cell*	Proliferation*	Tumor suppressor*	Novel	Others
Group 1: myeloid leukemia						
696	*Runx1*$^{-/-}$	*Gfi1/Evi5* (c)	*c-Myc* (c)			
807	*Runx1*$^{-/-}$		*Ncoa2*‡	*Ing4*		*Rbm34*
966	*Runx1*$^{-/-}$	*Evi1* (c)	*IL6st*			
714	*Runx1*$^{-/-}$	*Gfi1/Evi5* (c)	*Cyclin D3* (c), *Cyclin D2* (c)	*Dab2*‡		*Lfng*, *Swap70*
708	*Runx1*$^{-/-}$	*Evi1* (c)	*Pik3cd*	*Mapk9* (Jnk)	*Slis7* (c)	*Tmem23*‡
Group 2: biphenotypic leukemia						
691†	*Runx1*$^{-/-}$					
813	*Runx1*$^{-/-}$	*Gfi1/Evi5* (c)‡			*Slis6* (c)	*Arhgap25*
775	*Runx1*$^{-/-}$		*c-Myc* (c)			*Gimap7*, *Ak1*
770	*Runx1*$^{-/-}$		*Cyclin D3* (c), *Sema4d*	*Gadd45*	*Slis7* (c)	*Cspg4*, mSin3a
641	*Runx1*$^{-/-}$		*Cyclin D3* (c), *Cyclin D2* (c)	*Stag1*§	*Slis8* (c)	*Ang 2*
819	*Runx1*$^{-/-}$	*Gfi1/Evi5* (c)				*Stx4a*, *Negr1*
821	*Runx1*$^{-/-}$					
779	*Runx1*$^{-/-}$		*c-Myc* (c)	*Nkd1*	*Slis8* (c)	
982	*Runx1*$^{-/-}$	Gfi1/Evi5 (c)		*Stag1*§	*Slis6* (c)	*Limk2*
972	*Runx1*$^{-/-}$					*Ppfibp1*
969	*Runx1*$^{-/-}$	*Gfi1/Evi5* (c), *Evi1* (c)	*N-myc* (c)‡, *Cyclin D1* (c)	*Mad1l1*‡		*Rabggtb*
948	*Runx1*$^{-/-}$	*Gfi1/Evi5* (c)	*N-myc* (c)‡			*Stk16*, *Mdm4*
974	*Runx1*$^{-/-}$	*Lmo2*‖	*c-Myc* (c), *Cyclin D3* (c), *Lef1*			*Ldb1*
693	*Runx1*$^{+/+}$		*Tnfrsf191*	*Tspan32*		
690	*Runx1*$^{+/+}$	*Lmo2*‖		*Foxp1*		
663	*Runx1*$^{+/+}$	*Gfi1/Evi5* (c)	*Pip5k2a*‡			*Ugcg*
Unclassified‡						
2	*Runx1*$^{-/-}$	*Gfi1/Evi5* (c)	*N-myc* (c)‡, *Sept9*, *Pim2*			
4	*Runx1*$^{-/-}$	*Gfi1/Evi5* (c)‡, *Hes1*	*IL2*		*Slis6* (c)	*Birc4*
998	*Runx1*$^{-/-}$	*Gfi1/Evi5* (c)				
838	*Runx1*$^{-/-}$	*Gfi1/Evi5* (c)‡				

Table shows the genes near CISs or RISs that may have a role in oncogenesis based on their known or predicted function. (c) indicates CISs identified in this study. Leukemia cases in each group are arranged in ascending order of latency.

*Known or predicted function.

†RIS information is not available for this sample.

‡Genes with retroviral integrations inside the gene.

§Unclassified leukemia cases, which could belong to group 1 or 2; they showed early onset of disease and no enlargement of thymus/lymph node, and flow cytometric data are not available.

‖Gene near 2 RISs that cannot be classified as CISs based on definition.

was isolated by FACS and subjected to the experiments. LTC-IC assay was carried out after 30 days' culture of transfected *Runx1*$^{-/-}$ and *Runx1*$^{+/+}$ immature cells (GFP$^+$c-Kit$^+$) on OP9 stromal cells. The plating efficiency (colony number) of *Runx1*$^{-/-}$ cells with overexpression of *EVI5* gene was prominently high while that of mock-transfected *Runx1*$^{-/-}$ cells or *EVI5*-transfected *Runx1*$^{+/+}$ cells was lost, suggesting that cells overexpressing *EVI5* maintain a higher number of stem cells than other combinations (Figure 5A-B). When replated after 30 days, *Runx1*$^{-/-}$ cells carrying *EVI5* also showed a significantly high number of cobblestone area forming cells (CAFCs; Figure 5C). Furthermore, colony assay and CAFC assay after 30 more days of culture of replated cells (total 60 days after initial transfection) still showed a high number of colonies and CAFCs in *Runx1*$^{-/-}$ cells overexpressing *EVI5*. *GFI1*- and *EVI1*-transfected *Runx1*$^{+/+}$ or *Runx1*$^{-/-}$ cells did not show any colony or CAFCs after 30 days of LTC (Figure 5A,C).

Morphologic analyses of cells after 30 and 60 days of LTC revealed that *Runx1*$^{-/-}$ cells overexpressing *EVI5* have immature cell morphology characterized by nucleus with fine chromatin and basophilic cytoplasm. *Runx1*$^{-/-}$ cells transfected with mock vector and *Runx1*$^{+/+}$ cells overexpressing *EVI5* showed differentiated mast cell and macrophage morphology after 30 days of LTC (Figure 5D).

Taken together, the overexpression of *EVI5* strongly cooperates with *Runx1*$^{-/-}$ status in maintenance and proliferation of stem cells, and overexpression of *GFI1* or *EVI1* does not show significant cooperation in the OP9 culture. However, colony replating assay showed modest cooperation between *Runx1*$^{-/-}$ status and *EVI1* overexpression (supplemental Figure 3A).

Overexpression of *EVI5* and *EVI1* prevents exhaustion of *Runx1*$^{-/-}$ stem cells in vivo

To assess the in vivo effect, *EVI5* transfected *Runx1*$^{-/-}$ or *Runx1*$^{+/+}$ cells were transplanted into sublethally irradiated (6 Gy) recipient mice. Recipients of *Runx1*$^{+/+}$ cells transfected with *EVI5* showed stable GFP chimerism throughout, from 6 weeks to 30 weeks after transplantation, with an average of 20% to 25%. However, the GFP chimerism of mice that underwent transplantation with *Runx1*$^{-/-}$ cells overexpressing *EVI5* increased progressively, with a mean value of 25% at 6 weeks and 50% at 30 weeks

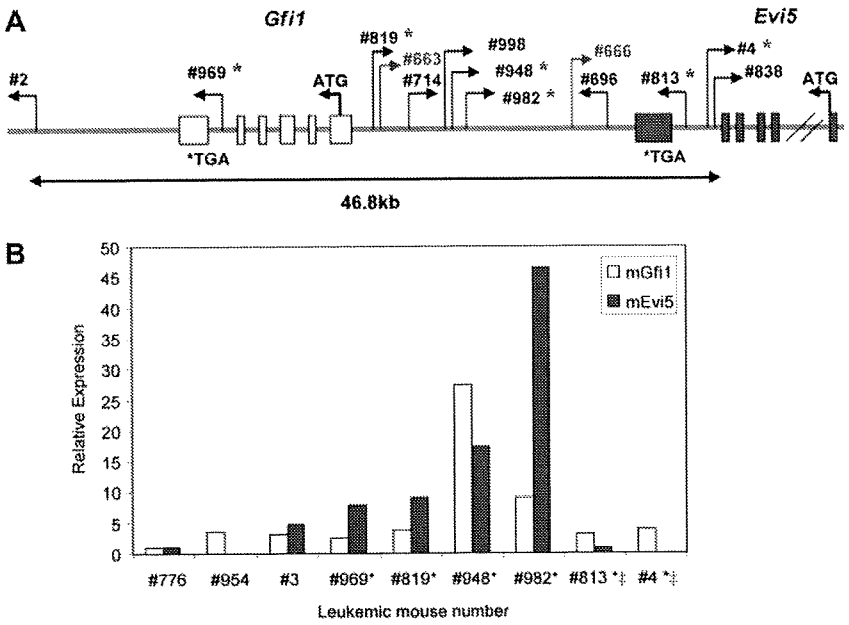

Figure 4. Frequent integrations at *Gfi1/Evi5* locus in *Runx1*$^{-/-}$ leukemias lead to overexpression of *Evi5*. (A) Schematic diagram of retroviral integration sites at *Gfi1/Evi5* locus in 2 *Runx1*$^{+/+}$ and 11 *Runx1*$^{-/-}$ leukemias. Numbers are unique to each leukemic mouse. Thin bent arrows represent the retrovirus integration site and its direction of integration. The 2 genes *Gfi* (light gray) and *Evi5* (dark gray) span from their initiation codons (ATG) to stop codons (TGA) with boxes representing exons. *Leukemia cases in which expression of *Gfi1* and *Evi5* was checked using qRT-PCR. (B) qRT-PCR analysis of *Gfi1* and *Evi5* expression in leukemic cells harboring integrations at *Gfi1/Evi5* locus (*), integrations within the *Evi5* gene (‡), and 3 control samples without integrations at this locus. Data are represented as fold change relative to control sample no. 776.

(Figure 5E). This is in contrast to the results seen after transplantation of mock vector–transfected *Runx1*$^{-/-}$ cells described earlier where the contribution of *Runx1*$^{-/-}$ cells to PB of recipient mice decreased progressively (Figure 1C). Thus, *EVI5* cooperates with *Runx1*$^{-/-}$ status in vivo also by preventing stem cell exhaustion and maintaining an increased number of *Runx1*-deficient stem cells. A secondary transplantation experiment was repeated to examine whether *EVI5* overexpression in *Runx1*$^{-/-}$ cells could rescue the defects in long-term repopulating abilities of *Runx1*$^{-/-}$ stem cells. Contrary to the previous results where 60% of the secondary recipients of *Runx1*$^{-/-}$ cells died within 3 months, all the secondary recipients of *Runx1*$^{-/-}$ cells overexpressing *EVI5* were alive (Figure 5F). We conclude that *EVI5* overexpression in *Runx1*$^{-/-}$ cells can prevent stem cell exhaustion of these cells and render them capable of reconstituting hematopoiesis in the secondary recipients.

As colony replating assay showed mild cooperation between *EVI1* overexpression and *Runx1*$^{-/-}$ status (supplemental Figure 3A), BMT was carried out for *EVI1* overexpressing cells as well. Recipients of *Runx1*$^{+/+}$ and *Runx1*$^{-/-}$ cells transfected with *EVI1* showed stable GFP chimerism throughout, from 6 weeks to 30 weeks after transplantation, with no significant increase or decrease in GFP chimerism (supplemental Figure 3B). Thus, *EVI1* overexpression also seems to rescue *Runx1*$^{-/-}$ stem cell exhaustion in vivo.

EVI5 is overexpressed in 44% of human patients with AML M2 RUNX leukemia

To evaluate whether *EVI5* overexpression synergizes with loss-of-function of RUNX1 in human patients with RUNX1-related leukemia, we carried out qRT-PCR on cDNA from patient samples with AML M2 carrying *RUNX1-ETO* fusion gene or AML M4Eo carrying *CBFB-MYH11* fusion gene. These fusion genes are more commonly found *RUNX1* alterations and they lead to loss-of-function of RUNX1. Expression of *EVI5* in other AML and CML samples without known RUNX1 alterations was also analyzed. cDNA from BM of 3 patients who had undergone complete remission was used as control. Indeed, very significant overexpression of *EVI5* was seen in 4 of 9 (44%) AML M2 patients examined. AML M4Eo patients also showed 2- to 3-fold overexpression as compared with control samples and AML samples without RUNX1 alteration (Figure 6). Thus, *EVI5* overexpression and concomitant loss-of-function of RUNX1 are often observed in human RUNX1-related leukemia cases, especially in AML M2 carrying *RUNX1-ETO* fusion gene, suggesting that EVI5 is likely to prevent stem cell exhaustion in human RUNX1-related leukemias.

Runx1$^{-/-}$ stem cell exhaustion may be due to defective interaction with the niche

Interaction of stem cells with the stem cell niche is important for maintaining the integrity and self-renewal properties of stem cells.[32,33] Analysis of a panel of niche-related factors in immature cell fraction (c-Kit^{+}GFP^{+}) of MIG vector–transfected *Runx1*$^{+/+}$ and *Runx1*$^{-/-}$ BM cells, revealed that one of the most important molecules for interaction with the stem cell niche, Cxcr4, was down-regulated in *Runx1*$^{-/-}$ cells. However, normal level of Cxcr4 expression was restored after overexpression of *EVI5* in *Runx1*$^{-/-}$ cells (supplemental Figure 4A). The down-regulation of Cxcr4 expression in the *Runx1*$^{-/-}$ stem/progenitor (KSL) cell fraction was further confirmed by flow cytometry ($P < .001$) and qRT-PCR ($P < .005$) (Figure 7A). Cxcr4 expression was also down-regulated in wild-type immature (c-Kit^{+}) BM cells transfected with the dominant-negative chimeric gene *RUNX1-ETO*, indicating that niche interaction may be altered in human RUNX1-related leukemic cases (Figure 7B). The qRT-PCR result indicates transcriptional regulation of *Cxcr4* expression by Runx1. Indeed, 2 RUNX binding sites are present in the *CXCR4* promoter region, and luciferase assay using the *CXCR4* promoter region showed that RUNX1 transactivates *CXCR4* more than 20-fold, in a DNA binding–dependent manner (Figure 7C). Along with Cxcr4, another niche interacting factor, CD49b, which is an α2 integrin, was also down-regulated in immature *Runx1*$^{-/-}$ cells and its expression restored to normal after overexpression of *EVI5* in these cells (supplemental Figure 4A).

We carried out a homing assay to evaluate whether *Runx1*$^{-/-}$ BM cells are compromised in homing and niche interaction. Five million BM cells from *Runx1*$^{+/+}$ and *Runx1*$^{-/-}$ mice were labeled with 100% efficiency by CFSE, and transplanted into recipient mice. Analysis of recipient BM 16 hours after transplantation revealed that *Runx1*$^{-/-}$ cells traffic to the BM with significantly reduced efficiency (Figure 7D, supplemental Figure 4B). Thus,

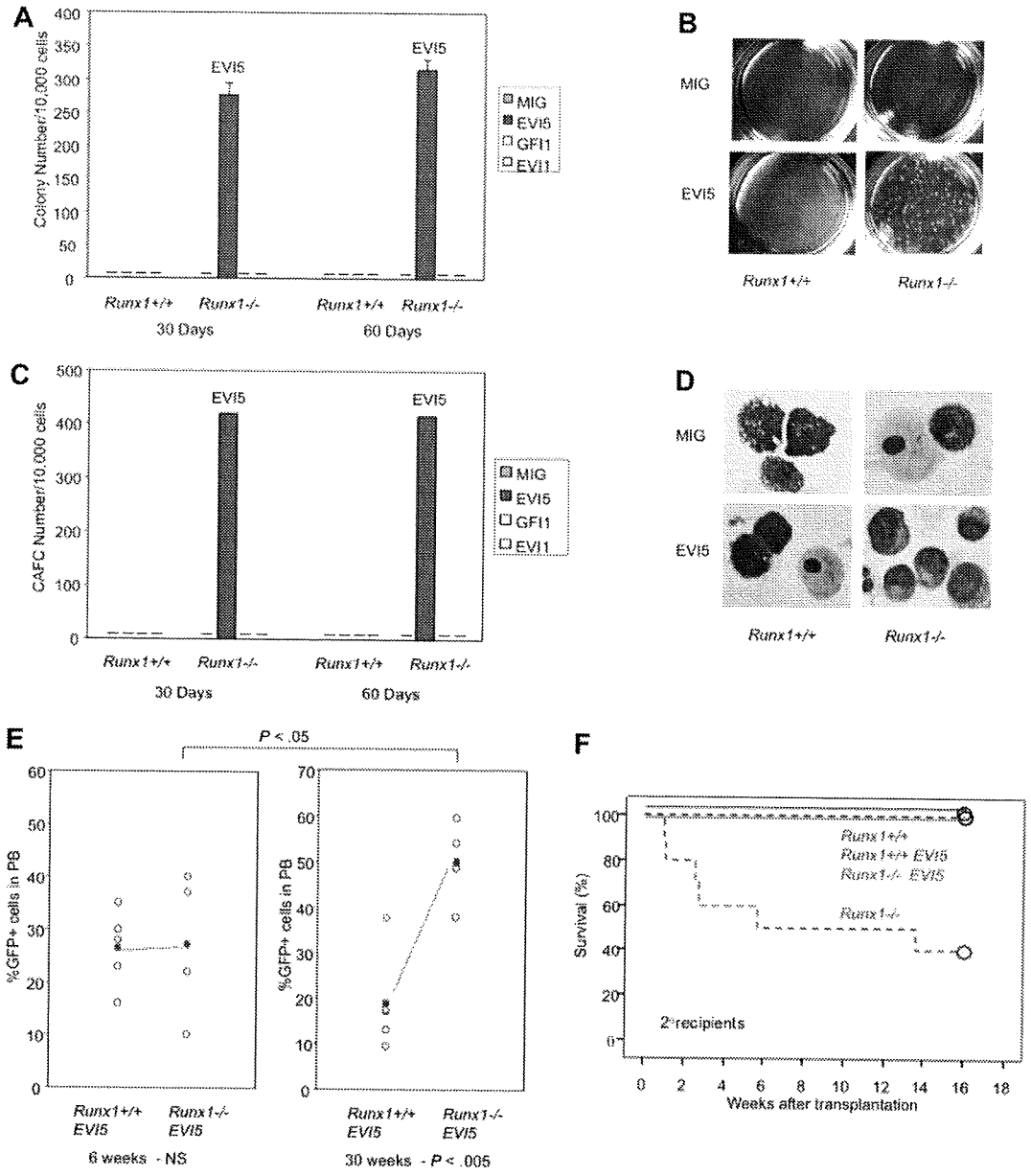

Figure 5. EVI5 overexpression and *Runx1*$^{-/-}$ status synergize in long-term maintenance of stem cells in vitro and in vivo. Graphic representation of (A) colony assay and (C) CAFC assay of immature cells from *Runx1*$^{+/+}$ and *Runx1*$^{-/-}$ BM cells transfected with mock MIG vector, *EVI5*, *GFI1*, or *EVI1*, after 30 and 60 days of long-term culture. Pictures of (B) colonies and (D) morphology of cells after 30 days of long-term culture. (E) GFP chimerism in recipients of *Runx1*$^{+/+}$ (n = 5) and *Runx1*$^{-/-}$ (n = 4) BM cells transfected with *EVI5*, 6 and 30 weeks after transplantation. Each open circle represents data from an individual mouse and the closed red circle is the average of a cohort. Statistical difference using unpaired Student *t* test is given at the bottom and on top. NS indicates not significant. (F) Kaplan-Meier survival curves of secondary recipients of *Runx1*$^{+/+}$ (blue; n = 4) and *Runx1*$^{-/-}$ (red; n = 4) BM cells transfected with mock MIG vector (dashed line) or MIG vector carrying *EVI5* (solid line). Circles represent end point of analysis.

altered ability to home and attach to the stem cell niche in the BM may be one of the reasons for *Runx1*$^{-/-}$ stem cell exhaustion.

To assess whether defects in niche interaction of Runx1-deficient HSCs lead to mobilization of stem/progenitor cells to the PB and spleen, we carried out colony assay of PB and flow cytometry analysis of spleen cells from *Runx1*$^{-/-}$ and *Runx1*$^{+/+}$ mice. PB (20 μL) from each *Runx1*$^{-/-}$ mouse formed an average of 35 colonies while PB from *Runx1*$^{+/+}$ mice did not form any colonies (Figure 7E). Similarly, a significantly higher number of stem/progenitor cells was present in the spleen of *Runx1*$^{-/-}$ mice (Figure 7F). These results indicate that Runx1 deficiency leads to dramatic egress of HSCs from the BM into the PB and spleen.

We also carried out a BrdU incorporation assay to analyze whether there is increased proliferation of HSC compartment of *Runx1*$^{-/-}$ mice due to their defective niche interaction and increased cell-cycle entry. As shown in Figure 7G, proliferation of stem/progenitor cells (KSL fraction) was strongly induced in *Runx1*$^{-/-}$ mice, resulting in approximately 7-fold more BrdU^{+} stem/progenitor cells in *Runx1*$^{-/-}$ mice ($P < .05$). Taken together, all the above results suggest that the interaction between *Runx1*$^{-/-}$ HSC and its niche may be perturbed, probably due to reduced expression of Cxcr4, resulting in the release of stem cells from the niche, leading to initial expansion and subsequent exhaustion of HSCs (supplemental Figure 5B).

Finally, expression of several genes involved in stem cell function and apoptosis were checked in immature (c-Kit^{+}) cell fraction of mock- or *EVI5*-transfected (GFP^{+}) BM cells from *Runx1*$^{+/+}$ and *Runx1*$^{-/-}$ mice, by qRT-PCR. Among the candidate genes tested, *Bmi-1*, important for self-renewal of normal and cancer stem cells,[34] and the antiapoptotic gene, *Bcl2*, which is negatively regulated by Runx family,[35,36] were overexpressed in

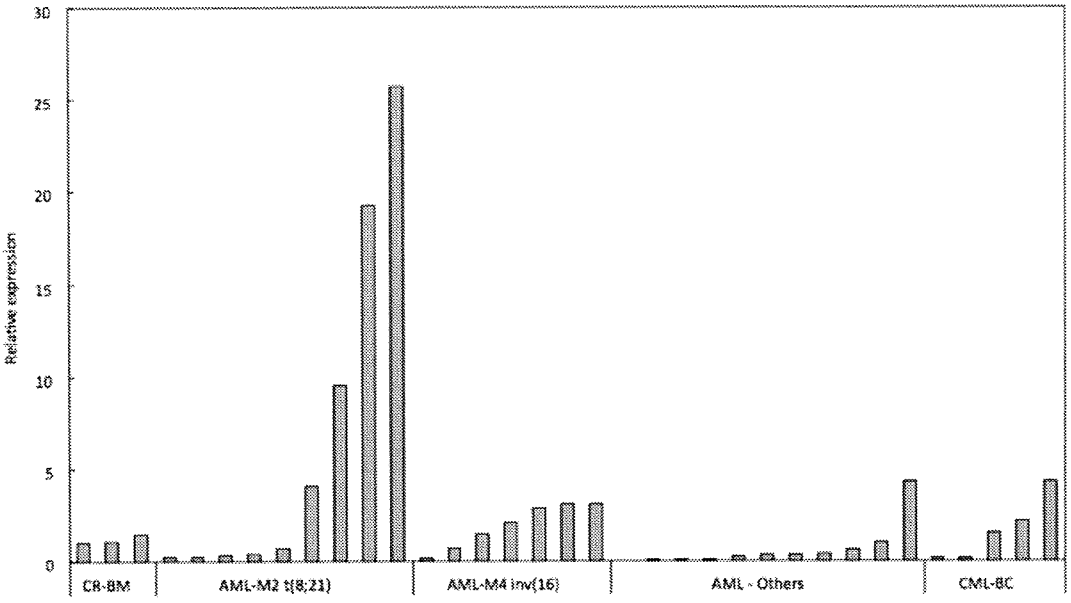

Figure 6. EVI5 is overexpressed in human RUNX leukemia. qRT-PCR analysis of *EVI5* expression in human RUNX1-related leukemia samples: AML M2 with t(8;21) resulting in RUNX1-ETO fusion protein, AML M4 with inv(16) resulting in PEBP2β-SMMHC fusion protein, other AML cases without *RUNX1* alteration and CML cases with blast crisis (CML-BC). Data are represented as fold change relative to BM samples undergoing complete remission (CR-BM).

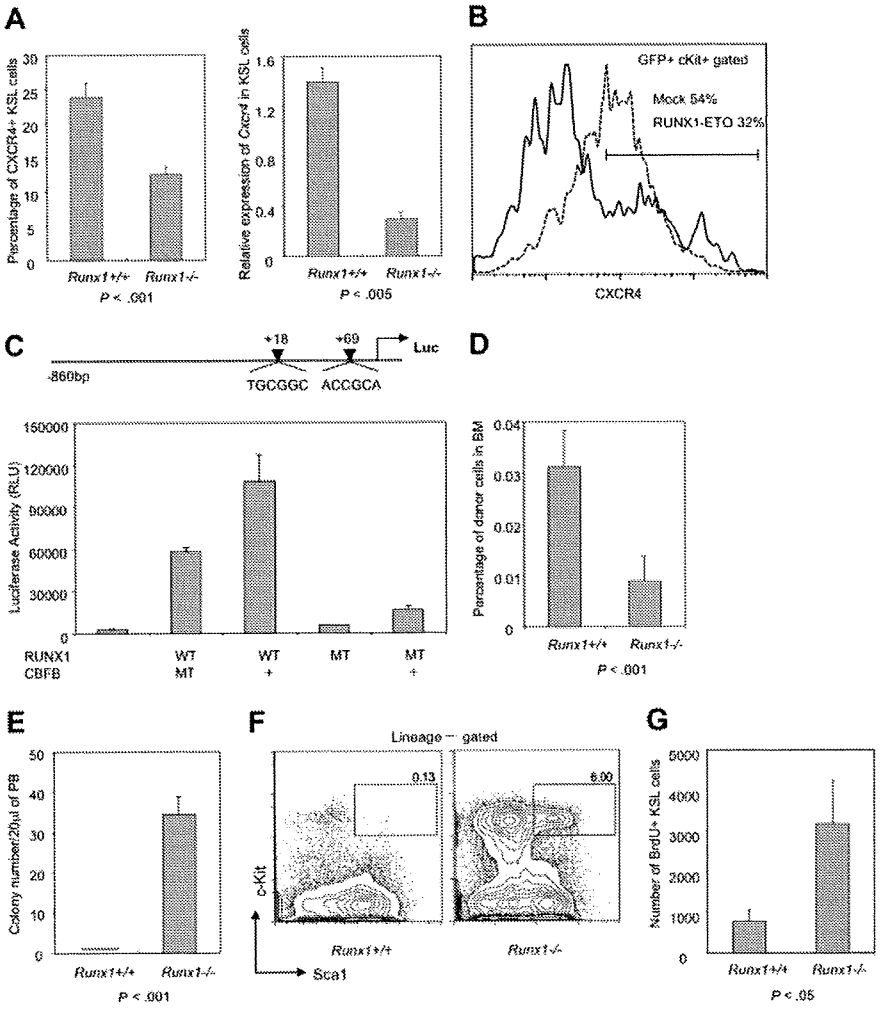

Figure 7. Decreased expression of niche factor, Cxcr4, and impaired homing may be responsible for *Runx1*$^{-/-}$ stem cell exhaustion. (A) Left panel: flow cytometric analysis of Cxcr4 expression on KSL cells from *Runx1*$^{+/+}$ (n = 4) and *Runx1*$^{-/-}$ (n = 3) mice. Right panel: qRT-PCR analysis of expression of *Cxcr4* in KSL fraction of *Runx1*$^{+/+}$ and *Runx1*$^{-/-}$ BM cells. Statistical difference using unpaired Student *t* test is given at the bottom. (B) Expression of Cxcr4 in c-Kit^{+}GFP^{+} cells from wild-type BM cells transfected with mock MIG vector (dashed line) or *RUNX1-ETO* (solid line). One representative result of 2 experiments is shown. (C) Structure of the CXCR4 promoter luciferase reporter construct. The 2 arrowheads represent the positions of 2 consensus Runx1 binding sites on the human *CXCR4* promoter. Graph represents the result of luciferase assay, showing transcriptional activity of wild-type RUNX1 (WT) or its mutant form R174Q (MT) with (+) or without CBFB, on *CXCR4* promoter. (D) Graph showing percentage of CFSE-stained *Runx1*$^{+/+}$ or *Runx1*$^{-/-}$ BM cells found in the recipient BM (n = 4 and 6, respectively), 16 hours after transplantation. Statistical difference using unpaired Student *t* test is given at the bottom. (E) Graphic representation of colony assay of 20 µL of PB from *Runx1*$^{+/+}$ (n = 4) and *Runx1*$^{-/-}$ (n = 4) mice. (F) FACS analysis of spleen KSL fraction in *Runx1*$^{+/+}$ and *Runx1*$^{-/-}$ mice. One representative flow cytometry profile from 2 experiments is shown. (G) Graph showing absolute number of BrdU^{+} KSL cells per 1 million BM cells analyzed from *Runx1*$^{-/-}$ (n = 3) and *Runx1*$^{+/+}$ mice (n = 3). Statistical difference using unpaired Student *t* test is given at the bottom.

Runx1$^{-/-}$ cells,[18] and the expression of these genes was further enhanced by overexpression of *EVI5* (data not shown).

Discussion

Loss-of-function of RUNX1 is frequently observed in human leukemia, implying that RUNX1 deficiency may predispose cells to leukemia development. Consistently, our previous study revealed that there is an expansion of the HSC/progenitor compartment in *Runx1*$^{-/-}$ mice, accompanied by resistance to cell death, senescence, and differentiation, characteristic of a leukemia-susceptible status.[18] Three other groups, who generated conditional *Runx1* knockout mice independently, also reported the expansion of the HSC/progenitor population.[15-17,37] However, there is no spontaneous leukemia development in the Runx1-deficient mice. In this report, we show that the reason for this paradox may be exhaustion of Runx1-deficient HSCs over time. We provided strong evidence for exhaustion of *Runx1*$^{-/-}$ stem cells using limiting dilution and secondary transplantation experiments. A similar conclusion was reported by others using competitive transplantation experiment.[16] Ichikawa et al also suggested that there appears to be a distinct difference in HSC numbers soon after deletion of *Runx1* alleles (4 to 9 weeks) and over long periods of time, although they described only the initial phase expansion.[37]

In order to understand the mechanism of *Runx1*$^{-/-}$ stem cell exhaustion, we explored cell intrinsic changes and alterations in stem cell niche interaction. Immature *Runx1*$^{-/-}$ cells expressed higher levels of *Bmi1* and *Bcl2*,[18] and they maintained their inherent proliferative ability at 40 weeks of age and even 2 years after transplantation (Figure 2B,C). These results suggest a cell-intrinsic bias toward survival rather than exhaustion of *Runx1*$^{-/-}$ cells. On the other hand, niche interaction, which is essential for maintaining the functional integrity and quiescence of HSCs, was impaired in immature *Runx1*$^{-/-}$ cells as evidenced by reduced expression of Cxcr4 in the KSL fraction, defective homing, and mobilization of HSCs from BM into PB and spleen. Conditional *Cxcr4* knockout mice show a very similar egress of HSCs from BM to PB and spleen,[38] supporting the notion that Cxcr4 could be the downstream factor that affects the niche interaction of Runx1-deficient cells. Quiescent LT-HSCs are found attached to osteoblasts in the endosteal niche of the trabecular bone. Under the steady-state condition, these HSCs are forced to leave their original niche and migrate to another niche due to continuous bone turnover. When there are coexisting wild-type HSCs in the cell milieu, HSCs that lack Runx1 could be outcompeted in establishing adequate interaction with another niche, leading to their slow exhaustion (supplemental Figure 5C). Thus, problems in niche interaction would be a critical issue in leukemia development, particularly at the initial step, and a leukemia initiating clone, or preleukemic stem cells, with *Runx1* alteration have to overcome this selective disadvantage for leukemia progression.

RIM to identify cooperating genetic alterations revealed that *Runx1*$^{-/-}$ mice injected with retrovirus showed shorter latency of leukemia development, thus confirming the leukemic predisposition of *Runx1*$^{-/-}$ status. There was a high frequency of stem cell–related genes affected in *Runx1*$^{-/-}$ mice and *EVI5* overexpression showed the most significant effect in rescuing stem cell exhaustion, followed by *EVI1* overexpression. Our results show that *EVI5* may rescue *Runx1*$^{-/-}$ stem cell exhaustion by restoring expression of Cxcr4 and CD49b (supplemental Figure 4A), which enables HSCs to home back and establish adequate interaction with the niche. It is well known that factors such as CXCR4 and CD44, which mediate homing and interaction with the stem cell niche, are often up-regulated in leukemia and are essential for maintenance of leukemic stem cells.[39-41] Thus, the ability of EVI5 to restore Runx1-deficient HSC interaction with its niche, together with other intrinsic factors, may be an important mechanism to rescue stem cell exhaustion, maintain leukemia-initiating stem cells, and promote leukemogenesis. It is not known how EVI5 mediates this effect. The role of EVI5 in the cell cycle may result in the indirect effects seen in HSC/progenitors since cell-cycle regulation is tightly linked to stem cell maintenance. Alternatively, EVI5 contains a conserved GAP domain, which has been shown to be important for actin cytoskeleton reorganization. Hematopoietic stem/progenitor cells from knockout mice of *Cdc42GAP*, one of the GAP domain family genes, showed impaired cortical F-actin assembly, deficiency in adhesion and migration, and defective homing and engraftment in the stem cell niche, leading to decline in stem cells.[42] EVI5 might play a similar role as Cdc42GAP and mediate homing and engraftment of Runx1-deficient HSCs through its GAP domain.

The recipient mice that underwent transplantation with *Runx1*$^{-/-}$ cells overexpressing *EVI5* or *EVI1* did not develop leukemia even 1 year after BMT, although the stem cell exhaustion was definitely rescued (Figure 5E-F, supplemental Figure 3B). Further genetic changes, such as strong mitogenic stimuli, are considered to be required for overt leukemia. Indeed, overexpression of oncogenes such as *c-Myc*, *N-Myc*, or *D-type cyclins* that promote cell proliferation was concurrently seen in 5 of 8 *Runx1*$^{-/-}$ leukemia cases showing *Evi5* overexpression in the RIM study (Table 2). In human RUNX1-related leukemia, similar mitogenic events such as mutations in receptor tyrosine kinases including *c-KIT* and *RAS* have been previously reported.[4,18] In fact, of the 4 human AML M2 cases carrying *RUNX1-ETO* which showed overexpression of *EVI5*, 3 cases had concurrent activating mutations in *c-KIT* or *FLT3*. Thus, these genetic alterations overlap with each other and act as second and third hits in RUNX1-related leukemia. Interestingly, mitogenic stimuli such as oncogenic Ras are shown to induce apoptosis, senescence, and differentiation, all of which function as negative factors for oncogenesis, and are considered as a vital cellular fail-safe mechanism. However, these detrimental effects due to oncogene stimulation are attenuated by Runx1-deficient status in the development of leukemia.[18] Similarly, negative effect of Runx1 deficiency, stem cell exhaustion, is in turn rescued by overexpresssion of *Evi5* and *Evi1*.

Considering the genes that are altered with high frequency in Runx1-related leukemias and the known properties and functions of these genes, we propose the following mechanism of Runx1-related leukemogenesis. Loss-of-function of Runx1 results in increase of stem/progenitor cell fraction and therefore serves as the target cell pool for leukemia. However, maintenance of *Runx1*$^{-/-}$ stem cells is compromised, probably due to the defect in interaction between HSC and niche, resulting in stem cell exhaustion. Overexpression of stem cell–related gene like *Evi5* rescues exhaustion of Runx1-deficient stem cells and maintains a significantly expanded pool of the aberrant cells with enhanced stem cell properties. Mitogenic stimuli such as activation of *c-Myc*, *N-myc*, *D-type cyclins*, *Ras*, or *c-Kit* result in overt proliferation of Runx1-deficient cells due to attenuated cellular fail-safe mechanism, thus providing the necessary stimulus for Runx1-deficient cells to develop full-blown leukemia. Such cooperative mechanism may be generally seen in cancer development whereby negative aspects caused by certain oncogenic hits are overcome by the others. Elucidation of these combinatorial mechanisms would provide profound insights into the understanding of oncogenesis and may provide a novel direction for therapeutic applications.

Acknowledgments

We thank M. Yanagida, L. Motoda, E. L. Ng, S. S. Nah, L. Q. Chen, and Q. R. Gwee for technical assistance and scientific discussions; N. Copeland and N. Jenkins for the MoMuLV retrovirus; M. Sugai for the MIG retroviral vector; G. P. Nolan for the Phoenix-Eco cell line; K. Morishita for human EVI1 cDNA; K. Rajewsky for Mx-Cre Tg mice; W. Krek for *CXCR4* promoter luciferase constructs; and members of the Biological Resource Center, Biopolis, for mouse husbandry.

This work was supported by A*STAR (Agency of Science, Technology and Research), Singapore National Research Foundation, and the Ministry of Education under the Research Center of Excellence Program.

Authorship

Contribution: B.J. and M.O. designed and performed experiments, analyzed data, and wrote the manuscript; N.Y. and C.Q.W. performed experiments; I.T. and D.R.L. provided the conditional *Runx1* knockout mice; N.A. provided the patient leukemic samples; and Y.I. analyzed data and contributed to writing the manuscript.

Conflict-of-interest disclosure: The authors declare no competing financial interests.

Correspondence: Motomi Osato or Yoshiaki Ito, Institute of Molecular and Cell Biology, 61 Biopolis Dr, Singapore 138673; e-mail: motomi@imcb.a-star.edu.sg or itoy@imcb.a-star.edu.sg.

References

1. Ito Y. RUNX genes in development and cancer: regulation of viral gene expression and the discovery of RUNX family genes. *Adv Cancer Res.* 2008;99:33-76.
2. Okuda T, van DJ, Hiebert SW, Grosveld G, Downing JR. AML1, the target of multiple chromosomal translocations in human leukemia, is essential for normal fetal liver hematopoiesis. *Cell.* 1996;84(2):321-330.
3. Wang Q, Stacy T, Binder M, et al. Disruption of the Cbfa2 gene causes necrosis and hemorrhaging in the central nervous system and blocks definitive hematopoiesis. *Proc Natl Acad Sci U S A.* 1996;93(8):3444-3449.
4. Speck NA, Gilliland DG. Core-binding factors in haematopoiesis and leukaemia. *Nat Rev Cancer.* 2002;2(7):502-513.
5. Castilla LH, Wijmenga C, Wang Q, et al. Failure of embryonic hematopoiesis and lethal hemorrhages in mouse embryos heterozygous for a knocked-in leukemia gene CBFB-MYH11. *Cell.* 1996;87(4):687-696.
6. Yergeau DA, Hetherington CJ, Wang Q, et al. Embryonic lethality and impairment of haematopoiesis in mice heterozygous for an AML1-ETO fusion gene. *Nat Genet.* 1997;15(3):303-306.
7. Song WJ, Sullivan MG, Legare RD, et al. Haploinsufficiency of CBFA2 causes familial thrombocytopenia with propensity to develop acute myelogenous leukaemia. *Nat Genet.* 1999;23(2):166-175.
8. Osato M, Asou N, Abdalla E, et al. Biallelic and heterozygous point mutations in the runt domain of the AML1/PEBP2alphaB gene associated with myeloblastic leukemias. *Blood.* 1999;93(6):1817-1824.
9. Osato M. Point mutations in the RUNX1/AML1 gene: another actor in RUNX leukemia. *Oncogene.* 2004;23(24):4284-4296.
10. Preudhomme C, Renneville A, Bourdon V, et al. High frequency of RUNX1 bi-allelic alteration in acute myeloid leukemia (AML) secondary to familial platelet disorder (FPD). *Blood.* 2009; 113(22):5583-5587.
11. Okuda T, Cai Z, Yang S, et al. Expression of a knocked-in AML1-ETO leukemia gene inhibits the establishment of normal definitive hematopoiesis and directly generates dysplastic hematopoietic progenitors. *Blood.* 1998;91(9):3134-3143.
12. Castilla LH, Garrett L, Adya N, et al. The fusion gene Cbfb-MYH11 blocks myeloid differentiation and predisposes mice to acute myelomonocytic leukaemia. *Nat Genet.* 1999;23(2):144-146.
13. Rhoades KL, Hetherington CJ, Harakawa N, et al. Analysis of the role of AML1-ETO in leukemogenesis, using an inducible transgenic mouse model. *Blood.* 2000;96(6):2108-2115.
14. Yuan Y, Zhou L, Miyamoto T, et al. AML1-ETO expression is directly involved in the development of acute myeloid leukemia in the presence of additional mutations. *Proc Natl Acad Sci U S A.* 2001;98(18):10398-10403.
15. Ichikawa M, Asai T, Saito T, et al. AML-1 is required for megakaryocytic maturation and lymphocytic differentiation, but not for maintenance of hematopoietic stem cells in adult hematopoiesis. *Nat Med.* 2004;10(3):299-304.
16. Growney JD, Shigematsu H, Li Z, et al. Loss of Runx1 perturbs adult hematopoiesis and is associated with a myeloproliferative phenotype. *Blood.* 2005;106(2):494-504.
17. Putz G, Rosner A, Nuesslein I, Schmitz N, Buchholz F. AML1 deletion in adult mice causes splenomegaly and lymphomas. *Oncogene.* 2006; 25(6):929-939.
18. Motoda L, Osato M, Yamashita N, et al. Runx1 protects hematopoietic stem/progenitor cells from oncogenic insult. *Stem Cells.* 2007;25(12):2976-2986.
19. Jonkers J, Berns A. Retroviral insertional mutagenesis as a strategy to identify cancer genes. *Biochim Biophys Acta.* 1996;1287(1):29-57.
20. van Lohuizen M, Verbeek S, Scheijen B, et al. Identification of cooperating oncogenes in E mu-myc transgenic mice by provirus tagging. *Cell.* 1991;65(5):737-752.
21. Nakamura T. Retroviral insertional mutagenesis identifies oncogene cooperation. *Cancer Sci.* 2005;96(1):7-12.
22. Yamashita N, Osato M, Huang L, et al. Haploinsufficiency of Runx1/AML1 promotes myeloid features and leukaemogenesis in BXH2 mice. *Br J Haematol.* 2005;131(4):495-507.
23. Yanagida M, Osato M, Yamashita N, et al. Increased dosage of Runx1/AML1 acts as a positive modulator of myeloid leukemogenesis in BXH2 mice. *Oncogene.* 2005;24(28):4477-4485.
24. Goemans BF, Zwaan CM, Miller M, et al. Mutations in KIT and RAS are frequent events in pediatric core-binding factor acute myeloid leukemia. *Leukemia.* 2005;19(9):1536-1542.
25. Taniuchi I, Osato M, Egawa T, et al. Differential requirements for Runx proteins in CD4 repression and epigenetic silencing during T lymphocyte development. *Cell.* 2002;111(5):621-633.
26. Kuhn R, Schwenk F, Aguet M, Rajewsky K. Inducible gene targeting in mice. *Science.* 1995; 269(5229):1427-1429.
27. Akagi K, Suzuki T, Stephens RM, Jenkins NA, Copeland NG. RTCGD: retroviral tagged cancer gene database. *Nucleic Acids Res.* 2004;32:D523-D527.
28. Hock H, Hamblen MJ, Rooke HM, et al. Gfi-1 restricts proliferation and preserves functional integrity of haematopoietic stem cells. *Nature.* 2004;431(7011):1002-1007.
29. Eldridge AG, Loktev AV, Hansen DV, et al. The evi5 oncogene regulates cyclin accumulation by stabilizing the anaphase-promoting complex inhibitor emi1. *Cell.* 2006;124(2):367-380.
30. Du Y, Spence SE, Jenkins NA, Copeland NG. Cooperating cancer-gene identification through oncogenic-retrovirus-induced insertional mutagenesis. *Blood.* 2005;106(7):2498-2505.
31. Yuasa H, Oike Y, Iwama A, et al. Oncogenic transcription factor Evi1 regulates hematopoietic stem cell proliferation through GATA-2 expression. *EMBO J.* 2005;24(11):1976-1987.
32. Moore KA, Lemischka IR. Stem cells and their niches. *Science.* 2006;311(5769):1880-1885.
33. Wilson A, Trumpp A. Bone-marrow haematopoietic-stem-cell niches. *Nat Rev Immunol.* 2006;6(2):93-106.
34. Iwama A, Oguro H, Negishi M, et al. Enhanced self-renewal of hematopoietic stem cells mediated by the polycomb gene product Bmi-1. *Immunity.* 2004;21(6):843-851.
35. Klampfer L, Zhang J, Zelenetz AO, Uchida H, Nimer SD. The AML1/ETO fusion protein activates transcription of BCL-2. *Proc Natl Acad Sci U S A.* 1996;93(24):14059-14064.
36. Frank RC, Sun X, Berguido FJ, Jakubowiak A, Nimer SD. The t(8;21) fusion protein, AML1/ETO, transforms NIH3T3 cells and activates AP-1. *Oncogene.* 1999;18(9):1701-1710.
37. Ichikawa M, Goyama S, Asai T, et al. AML1/Runx1 negatively regulates quiescent hematopoietic stem cells in adult hematopoiesis. *J Immunol.* 2008;180(7):4402-4408.
38. Sugiyama T, Kohara H, Noda M, Nagasawa T. Maintenance of the hematopoietic stem cell pool by CXCL12-CXCR4 chemokine signaling in bone marrow stromal cell niches. *Immunity.* 2006;25(6):977-988.
39. Krause DS, Lazarides K, von Andrian UH, Van Etten RA. Requirement for CD44 in homing and engraftment of BCR-ABL-expressing leukemic stem cells. *Nat Med.* 2006;12(10):1175-1180.
40. Jin L, Hope KJ, Zhai Q, Smadja-Joffe F, Dick JE. Targeting of CD44 eradicates human acute myeloid leukemic stem cells. *Nat Med.* 2006;12(10):1167-1174.
41. Tavor S, Petit I, Porozov S, et al. CXCR4 regulates migration and development of human acute myelogenous leukemia stem cells in transplanted NOD/SCID mice. *Cancer Res.* 2004;64(8):2817-2824.
42. Wang L, Yang L, Filippi MD, Williams DA, Zheng Y. Genetic deletion of Cdc42GAP reveals a role of Cdc42 in erythropoiesis and hematopoietic stem/progenitor cell survival, adhesion, and engraftment. *Blood.* 2006;107(1):98-105.

Leukemia (2009) 23, 2197–2209

www.nature.com/leu

LEADING ARTICLE

Mixed-lineage-leukemia (*MLL*) fusion protein collaborates with Ras to induce acute leukemia through aberrant *Hox* expression and Raf activation

R Ono[1,2,3], H Kumagai[1], H Nakajima[4,5], A Hishiya[1,2], T Taki[6], K Horikawa[7], K Takatsu[7,8], T Satoh[9], Y Hayashi[10], T Kitamura[2] and T Nosaka[1,2,3]

[1]*Division of Hematopoietic Factors, The Institute of Medical Science, The University of Tokyo, Tokyo, Japan;* [2]*Division of Cellular Therapy, The Institute of Medical Science, The University of Tokyo, Tokyo, Japan;* [3]*Department of Microbiology and Molecular Genetics, Mie University Graduate School of Medicine, Mie, Japan;* [4]*Center of Excellence, The Institute of Medical Science, The University of Tokyo, Tokyo, Japan;* [5]*Division of Hematology, Department of Internal Medicine, Keio University School of Medicine, Tokyo, Japan;* [6]*Department of Molecular Laboratory Medicine, Kyoto Prefectural University of Medicine Graduate School of Medical Science, Kamigyo-ku, Kyoto, Japan;* [7]*Department of Immunology, The Institute of Medical Science, The University of Tokyo, Tokyo, Japan;* [8]*Department of Immunobiology and Pharmaceutical Genetics, Graduate School of Medicine and Pharmaceutical Sciences, University of Toyama, Toyama, Japan;* [9]*Division of Molecular Biology, Department of Biochemistry and Molecular Biology, Kobe University Graduate School of Medicine, Kobe, Japan and* [10]*Gunma Children's Medical Center, Gunma, Japan*

***Mixed-lineage-leukemia* (*MLL*) fusion oncogenes are closely involved in infant acute leukemia, which is frequently accompanied by mutations or overexpression of *FMS-like receptor tyrosine kinase 3* (*FLT3*). Earlier studies have shown that *MLL* fusion proteins induced acute leukemia together with another mutation, such as an *FLT3* mutant, in mouse models. However, little has hitherto been elucidated regarding the molecular mechanism of the cooperativity in leukemogenesis. Using murine model systems of the *MLL*-fusion-mediated leukemogenesis leading to oncogenic transformation *in vitro* and acute leukemia *in vivo*, this study characterized the molecular network in the cooperative leukemogenesis. This research revealed that *MLL* fusion proteins cooperated with activation of Ras *in vivo*, which was substitutable for Raf *in vitro*, synergistically, but not with activation of signal transducer and activator of transcription 5 (STAT5), to induce acute leukemia *in vivo* as well as oncogenic transformation *in vitro*. Furthermore, *Hoxa9*, one of the *MLL*-targeted critical molecules, and activation of Ras *in vivo*, which was replaceable with Raf *in vitro*, were identified as fundamental components sufficient for mimicking *MLL*-fusion-mediated leukemogenesis. These findings suggest that the molecular crosstalk between aberrant expression of *Hox* molecule(s) and activated Raf may have a key role in the *MLL*-fusion-mediated-leukemogenesis, and may thus help develop the novel molecularly targeted therapy against *MLL*-related leukemia.**

Leukemia (2009) **23,** 2197–2209; doi:10.1038/leu.2009.177;
published online 27 August 2009
Keywords: MLL; Ras; MAP kinase; leukemogenesis

Introduction

Multistep oncogenesis has been suggested in malignancy by the observation of more than two heterogeneous genetic and/or epigenetic lesions.[1] In leukemogenesis, recurring chromosomal translocations are frequently found in hematological malignancies, which sometimes coincide with subtle but critical genetic mutations leading to functional aberration.[2–4] Earlier studies showed that many of the translocation target genes are transcription factors involved in hematopoietic differentiation and/or self-renewal, whereas coincident mutations often occur on the genes involved in cell proliferation.[4] These results lead to a hypothetical model of leukemogenesis in which these two kinds of genetic alterations may cooperate to induce acute leukemia. This concept has been recently exemplified in experimental models using combinations of fusion genes, including *mixed-lineage leukemia* (*MLL*, also called *ALL1* or *HRX*) or *AML1* fusion genes, and other coincident genetic mutations.[5–9]

MLL is a proto-oncogene that is rearranged in human acute leukemia with chromosome 11 band q23 (11q23) translocation,[10,11] encoding a histone methyltransferase that assembles in a chromatin-modifying supercomplex.[12] Meanwhile, *MLL* fusion gene leads to leukemogenesis through several *HOX* genes directly transactivated by *MLL* fusion protein itself.[4,11,13,14] It is noteworthy that most of the genetically engineered mice carrying the *MLL* fusion developed hematological malignancy after a long latency, suggesting that secondary genotoxic stress is required to develop overt acute leukemia.[15–18] An earlier study presented direct evidence that *MLL* fusion proteins induced myeloproliferative disease (MPD) with a long latency, and caused acute leukemia with a short latency together with a coincident mutation of *FMS-like tyrosine kinase 3* (*FLT3*).[6]

Recent studies revealed that genetic alterations, including *FLT3*, *NRAS* (neuroblastoma RAS viral (v-ras) oncogene homolog) and *KRAS* (v-Ki-ras2 Kirsten rat sarcoma viral oncogene homolog), are frequently accompanied by 11q23 translocation.[19,20] *FLT3* is a receptor tyrosine kinase involved in leukemogenesis and normal hematopoiesis.[21] The mutations of *FLT3* are mainly classified into length mutations such as internal tandem duplication (ITD) of the juxtamembrane domain, and point mutations within the activation loop of the second tyrosine kinase domain (TKD).[21] Interestingly, *FLT3*-TKD, as well as overexpression of the wild type of FLT3, is found to be frequently associated with infant acute lymphoid leukemia (ALL), with rearrangements of *MLL*.[19,22] Both types of *FLT3* mutations result in a constitutive activation of *FLT3* kinase activity, followed by activation of signaling pathways, including signal transducer and activator of transcription 5 (STAT5) and Ras/Raf/mitogen-activated protein (MAP) kinase.[23,24] Both STAT5 and Ras/Raf/MAP kinase (MAPK) are involved in cellular

Correspondence: Dr T Nosaka, Department of Microbiology and Molecular Genetics, Mie University Graduate School of Medicine, 2-174 Edobashi, Tsu, Mie 514-8507, Japan.
E-mail: nosaka@doc.medic.mie-u.ac.jp
Received 1 October 2008; revised 17 July 2009; accepted 21 July 2009; published online 27 August 2009

proliferation, survival and differentiation.[25,26] Constitutively active mutants of Ras induce oncogenic transformation through activation of the MAPK cascade.[26] However, little has so far been elucidated regarding the molecular mechanism of collaboration in leukemogenesis.

To further clarify the molecular mechanism of *MLL*-fusion-mediated leukemogenesis, we focused on signal transduction associated with malignant transformation that collaborates with *MLL* fusion protein *in vitro*, and highlighted the contrastive roles of STAT5 and MAPK in leukemogenesis. Interestingly, comparative analyses suggested synergistic collaboration with activated Ras in *MLL*-fusion-mediated leukemogenesis, and also activation of Raf in malignant transformation *in vitro*, but not with STAT5 activation *in vivo* and *in vitro*. Thus, the activation of Ras/Raf/MAPK cascade may have an important role in multistep leukemogenesis with 11q23 translocations.

Materials and methods

Construction of the plasmids and retrovirus production

Fragments of murine constitutively active mutants of STAT5A (#2[27] and 1*6[28]) fused with a FLAG tag at the C-terminus, a coding region of human *NRAS*^{G12V} and *MLL-eleven nineteen leukemia* (*ENL*) short form[6] were inserted upstream of the internal ribosomal entry site (IRES)-enhanced green fluorescent protein (EGFP) cassette of pMYs-IRES-EGFP.[29] Fragments of coding regions of a wild type of *NRAS* and *NRAS*^{G12V} were inserted into pMXs-puro.[29] A fragment of murine *Hoxa9*[30] (a kind gift from Dr G Sauvageau) was inserted into pMXs-IRES-EGFP.[29] A fragment of a dominant negative mutant (dn) of STAT5A[23] was inserted upstream of the IRES-Kusabira-Orange (KO)[31] cassette of pMXs-IRES-KO, in which the EGFP cassette in pMXs-IRES-EGFP[29] was replaced with the KO cassette of phKO1-S1 (MBL, Nagoya, Japan). pMXs-neo-*MLL-SEPT6*,[6] pMY-FLT3-ITD-IRES-EGFP,[6] pMY-FLT3^{D835V}-IRES-EGFP[6] and pBabe-puro-Δ*Raf*-estrogen receptor (ER)[28] were described earlier. Retroviruses were harvested 48 h after transfection with each retroviral construct into PlatE cells[29] in which appropriate expression of the transgenes was confirmed by western blot analysis, as described earlier.[6]

Cells

An *MLL-SEPT6*-immortalized murine myelomonocytic cell line, HF6, was established through colony-replating assays using retroviral transduction with pMXs-neo-*MLL-SEPT6* as described earlier.[6] A *Hoxa9*-immortalized murine myelomonocytic cell line, A9G, was established through infection with retroviruses harboring *Hoxa9* in pMXs/IRES-EGFP[29] as reported earlier.[32] The HF6,[6] A9G and murine pro-B Ba/F3[28] cells were cultured in the presence of interleukin-3 (IL-3) (R&D Systems, Minneapolis, MN, USA). HF6 cells transduced with *FLT3* mutants were cultured in the same medium, except for the absence of IL-3. The expression levels of *FLT3* in these cells were evaluated using a phycoerythrin (PE)-conjugated anti-CD135 antibody, or an anti-mouse immunoglobulin G1,κ, as the isotype-matched control (BD Biosciences, San Diego, CA, USA) using fluorescence-activated cell sorting (FACS) Calibur (BD Biosciences) as described earlier.[33]

Immunoprecipitation and western blot analysis

Fifty million parental and additionally transduced HF6 cells, or 10 million parental and transduced Ba/F3 cells, were harvested in the lysis buffer, and the lysates were either suspended with 1 × sodium dodecyl sulfate sample buffer after immunoprecipitation using polyclonal anti-STAT5A antibody (L-20) (Santa Cruz Biotechnology, Santa Cruz, CA, USA) or directly mixed with an equal volume of 2 × sodium dodecyl sulfate sample buffer and then boiled, as described earlier.[25] In some experiments, the parental HF6 cells had been deprived of IL-3 8 h before harvest. Western blot analysis of each sample was performed using the polyclonal anti-STAT5A (L-20), monoclonal anti-phosphotyrosine (4G10) (Upstate Biotechnology, Lake Placid, NY, USA), polyclonal anti-extracellular signal-related kinase (ERK)1/2, monoclonal anti-phospho-ERK1/2 (E10) (Cell Signaling Technology, Danvers, MA, USA), monoclonal anti-α-tubulin (Sigma-Aldrich, St Louis, MO, USA), monoclonal anti-FLAG (M2), polyclonal anti-ERα (MC-20) and monoclonal anti-N-Ras (F155) (Santa Cruz Biotechnology) antibodies to probe membranes, as described earlier.[25]

Evaluation of cellular effects by inhibition of signal transduction in vitro

The response to the drug was evaluated as described earlier.[23] In brief, HF6 cells expressing the *FLT3* mutants (3×10^5) were infected with retroviruses harboring or not harboring the dnSTAT5A in pMXs-IRES-KO in the presence of polybrene, as described earlier.[6] Viable cell numbers were counted with standard Trypan blue staining, and the expression of the dnSTAT5A was monitored by assessment of KO positivity using the FL2 channel on the FACS Calibur, daily after infection. At 48 h after infection, to evaluate the status of phosphorylated STAT5, half a million of these cells were fixed with fixation buffer, permeablized with Perm Buffer III and analyzed with an Alexa Fluor 647-conjugated anti-phospho-STAT5 (Y694) (all from BD Biosciences) antibody, or the anti-mouse immunoglobulin G1,κ, as the isotype-matched control antibody, using the FL4 channel on the FACS Calibur, according to the manufacturer's recommendation. As controls, the parental HF6 cells with and without IL-3 stimulation after deprivation of IL-3 for 8 h were used. Meanwhile, these HF6 cells (1×10^4) were cultured for 72 h in 24-well plates in the presence of various concentrations of a MAPK kinase (MEK) inhibitor, U0126, or a PI3 kinase inhibitor, LY294002 (Calbiochem-Novabiochem, San Diego, CA, USA) and each vehicle control (ethanol for U0126 and dimethyl sulfoxide for LY294002). Viable cell numbers were counted with standard Trypan blue staining after each treatment, followed by calculation of the 50% inhibitory concentration (IC50) of each drug using a logistic regression model. To evaluate the inhibitory effect of U0126 on ERK1/2, five million of the cells were treated for 2 h, harvested and analyzed with the anti-ERK1/2 or the anti phospho-ERK1/2 antibody after western blotting.

Myeloid transformation assays in vitro

In a series of transformation assays, the acquisition of IL-3-independent proliferation was examined in IL-3-dependent cells. HF6 and Ba/F3 cells were infected with retroviruses harboring *NRAS*, *NRAS*^{G12V} or mock in pMXs-puro; Δ*Raf*-ER or mock in pBabe puro; and STAT5A1*6, STAT5A#2 or none (only GFP) in pMYs-IRES-EGFP, respectively, in the presence of polybrene, as described earlier.[6] A9G cells were also retrovirally transduced with *NRAS*, *NRAS*^{G12V} Δ*Raf*-ER or each mock in the same way. For puromycin selection, the transduced cells were cultured with 1 μg/ml of puromycin 24–96 h after infection, followed by propagation for 5 days in the absence of puromycin.

Next, 1×10^5 puromycin-resistant cells transduced with *NRAS*, *NRAS*^{G12V} or mock were cultured in 24-well plates in the absence of IL-3, whereas those transduced with Δ*Raf*-ER or mock were cultured under the same condition, except for the presence of 1 μM of 4-hydroxy-tamoxifen or a vehicle control (ethanol). The cells transduced with STAT5A1*6, STAT5#2 or none were purified on the basis of the expression of GFP using a FACS Aria (BD Biosciences) 36 h after infection. Immediately, these purified cells (1×10^4) were cultured in 96-well plates in the absence of IL-3, to avoid excessive signals caused by STAT5A#2 or 1*6 in the presence of IL-3, which led to cell death as described earlier.[25] Viable cell numbers were counted periodically after standard Trypan blue staining.

Leukemogenesis assays in vivo

Leukemogenesis assays *in vivo* using C57BL/6 mice produced by a combination of two kinds of transgenes were performed with lethal conditioning using lethally (9.5 Gy) irradiated recipients, or with sublethal conditioning using sublethally (5.25 Gy) irradiated recipients receiving no radioprotective bone marrow (BM) cells, as described earlier[6] (Supplementary Figure 1). In brief, hematopoietic progenitors were harvested from 6- to 10-week-old Ly-5.1 C57BL/6 mice 4 days after intraperitoneal administration of 150 mg/kg 5-fluorouracil, and cultured overnight in alpha minimal essential medium supplemented with 20% fetal calf serum and 50 ng/ml each of mouse stem cell factor, human IL-6, human FLT3-ligand (R&D Systems) and human thrombopoietin (Kirin Brewery, Takasaki, Japan). The prestimulated cells were infected with several combinations of the retroviruses for 60 h in the α minimal essential medium supplemented with the same fetal calf serum and cytokines using RetroNectin (Takara Bio Inc., Otsu, Japan) according to the manufacturer's recommendations, followed by intravenous injection of 10^5 of the cells into Ly-5.2 mice together with either a radioprotective dose (2×10^5) of Ly-5.2 cells under lethal conditioning or none under sublethal conditioning. Morbid mice and their tissue samples were analyzed, and immunophenotyping of BM, splenic and thymic cells was performed using the FACS Calibur, as described earlier.[33] The hematopoietic neoplasms were diagnosed mainly on the basis of morphology as described earlier.[6] The probabilities of murine overall survival were estimated using Kaplan–Meier method and compared using the log-rank test. All animal studies were performed in accordance with the guidelines of the Animal Care Committees of the Institute of Medical Science, the University of Tokyo and the Mie University.

Southern blot analysis

Genomic DNA was extracted from spleens, digested with *Nhe*I or *Bam*HI for detecting proviral integration and clonality, respectively, and analyzed with the Neo or puro probe (Supplementary Figure 1) as described earlier.[34]

Reverse transcriptase-polymerase chain reaction (PCR)

Total RNA was extracted from cell lines, spleen or BM, and reverse transcribed to complementary DNA as described earlier.[6] The conditions, reagents for reverse transcriptase-PCR and the primers specific for *β*$_2$*microglobulin* (*β*$_2$*MG*), *Hoxa9* and *MLL-SEPT6* have been described earlier,[6] except that PCR amplification for *MLL-SEPT6* transcripts was sometimes run for 35 cycles. To detect the transcript of *NRAS*^{G12V}, PCR amplification was run for 21 cycles using the following primers: *NRAS-S*, 5′-GTGGTTATAGATGGTGAAACCTGTT-3′ and *NRAS-AS*, 5′-GACCATAGGTACATCTTCAGAGTCCT-3′.

Results

MLL-SEPT6 *cooperates with both types of* FLT3 *mutations through different modes of signal transduction*

To clarify the molecular mechanism of cooperation between *MLL* fusion proteins and *FLT3* mutants, signaling pathways of *FLT3*-ITD and *FLT3*-TKD that cooperate with *MLL-SEPT6* were examined using the IL-3-dependent *MLL-SEPT6*-immortalized cell line, HF6.[6] Earlier, STAT5 and MAPK ERK1/2 had been found to be activated downstream of *FLT3* mutants in factor-dependent cell lines.[23,24] Therefore, the activation of these molecules was first examined using parental HF6 and transformed HF6 cells expressing FLT3-*ITD* (HF6^{ITD}) or *FLT3*^{D835V} (HF6^{D835V}) described earlier.[6] Nearly equal levels of expression of the *FLT3* mutants in the transformed HF6 cells were confirmed (Figure 1a). A western blot analysis after immunoprecipitation of the lysates from these cells revealed constitutive phosphorylation of STAT5A in HF6 cells expressing the FLT3 mutants in the absence of IL-3, but little in the parental HF6 cells that had been deprived of IL-3 (Figure 1b). In addition, a western blot analysis of the same lysates also revealed constitutive phosphorylation of ERK1/2 in those cells expressing the *FLT3* mutants, but little in the parental HF6 cells that had been deprived of IL-3 (Figure 1b).

Next, to determine whether STAT5 and/or MAPK were important in the transformation of HF6 cells expressing *FLT3* mutants, each signaling pathway was inhibited using dnSTAT5A or MEK inhibitor U0126. After retroviral transduction with the dnSTAT5A, the proliferation of HF6^{ITD} cells expressing dnSTAT5A was suppressed more efficiently than that of HF6^{D835V} cells expressing dnSTAT5A (Figure 2a). KO-positive cells expressing dnSTAT5A showed higher levels of phosphorylated STAT5 than KO-negative cells (Figure 2b). This finding is consistent with the earlier report showing that the dnSTAT5A exerts its effect on endogenous STAT5A and 5B with persistent phosphorylation of the dnSTAT5A itself.[35] In contrast, U0126 retarded the proliferation of the HF6^{D835V} cells more effectively than the HF6^{ITD} cells (Figure 2c, each IC50 is 0.67 ± 0.35 μM for HF6^{D835V} and 6.09 ± 0.90 μM for HF6^{ITD} in the absence of IL-3). Indeed, U0126 inhibited phosphorylation of ERK1/2 in the HF6^{ITD} and HF6^{D835V} cells in a semidose-dependent manner (Figure 2d). In addition, another important signaling pathway downstream of *FLT3*, through PI3 kinase, was inhibited using LY294002. LY294002 also retarded the growth of the HF6^{D835V} and HF6^{ITD} cells in a dose-dependent manner, but there was no remarkable difference between both types of HF6 cells (Supplementary Figure 2, each IC50 is 4.18 ± 0.55 μM for HF6^{D835V} and 8.12 ± 1.54 μM for HF6^{ITD} in the absence of IL-3).

Taken together, these results *in vitro* suggested that the activation of MAPK was more critical for transformation by *FLT3*-TKD than by *FLT3*-ITD in HF6 cells, whereas activation of STAT5 was more critical for transformation by *FLT3*-ITD than by *FLT3*-TKD.

Activation of Ras-MAPK cascade enables HF6 cells to grow without IL-3 through cooperation between Hoxa9 *and Raf*

We further examined whether direct activation of either STAT5 or MAPK cascade is sufficient to confer factor-independent

growth on HF6 cells. Although the constitutively active mutants of STAT5A, the relatively stronger mutant STAT5A1*6 and weaker mutant STAT5A#2, enabled Ba/F3 cells (Ba/F3^{1*6}, Ba/F3$^{\#}$) to grow without IL-3 as reported earlier,[25,27,28] both failed to confer factor-independent growth on HF6 cells with limited elongation of survival time without IL-3 (Figures 3a and c). In contrast, the oncogenic *NRAS* mutant, *NRAS*^{G12V}, which had been detected in a case of *AML* with *MLL-SEPT6*,[20] enabled HF6 cells (HF6^{G12V}) to grow without IL-3, while it conferred no factor-independent growth on Ba/F3 with limited elongation of survival time without IL-3 (Figures 3b and c). In addition, Raf-1, a signal molecule downstream of Ras in Ras-MAPK cascades associated with malignant transformation, was tested with an activation-inducible system using Δ*Raf*-ER, consisting of the catalytic domain of human RAF-1 (ΔRaf) and the hormone-binding domain of the ER (Figure 3d), as described earlier.[28] Unlike transduced Ba/F3 (Ba/F3$^{\Delta Raf\text{-}ER}$) cells, transduced HF6 (HF6$^{\Delta Raf\text{-}ER}$) cells grew without IL-3 only in the presence of 4-hydroxy-tamoxifen (Figure 3e). In these HF6$^{\Delta Raf-ER}$ cells treated with 4-hydroxy-tamoxifen, STAT5A was not found to be secondarily activated by induction of activation of Raf/MAPK cascade in the absence of IL-3, whereas it was found to be weakly activated by stimulation with IL-3 for 15 min (data not shown).

Furthermore, we examined whether *Hoxa9*, which is one of the well-known target genes of *MLL* fusion proteins,[10,11,13,14] is involved in cooperation between *MLL* fusion protein and Ras/Raf/MAPK cascade. In the myeloid transformation assays, the murine BM progenitors immortalized by *Hoxa9* in the presence of IL-3 (named A9G) proliferated without IL-3 after retroviral transduction of *NRAS*^{G12V} (Figure 3b). In the inducible transformation system using Δ*Raf*-ER, transduced A9G

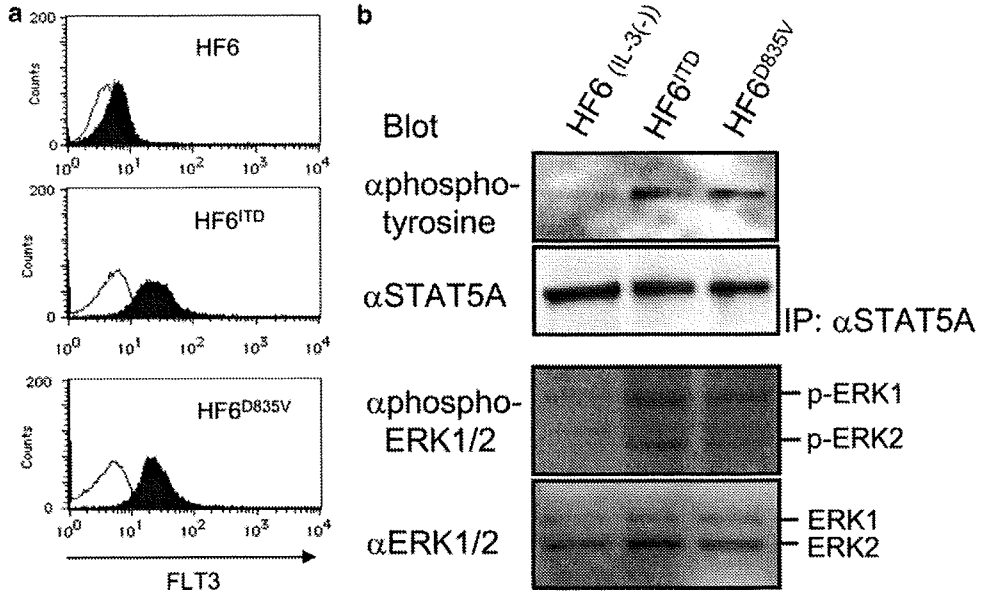

Figure 1 Characterization of signal transduction in the HF6 cells transformed by *FMS-like receptor tyrosine kinase 3* (*FLT3*) mutants. (**a**) Expression of each *FLT3* mutant in HF6 and their transformed cells. The shadow profiles and black lines represent fluorescence-activated cell sorting (FACS) staining obtained using the antibody specific to *FLT3* and its isotype control antibody, respectively. (**b**) Western blot analyses of proteins extracted from HF6 and their transformed cells after immunoprecipitation using the anti-signal transducer and activator of transcription 5A (STAT5A) antibody (upper two panels), and of the whole lysates (lower two panels). The parental HF6 cells had been deprived of interleukin-3 (IL-3) 8 h before harvest. The blot of the immunoprecipitated samples was probed with the anti-STAT5A antibody (upper bottom panel), followed by reprobe with 4G10 (the anti-phosphotyrosine antibody) (upper top panel). The blot of the whole lysates was probed with the anti-extracellular signal-related kinase (ERK)1/2 antibody (lower bottom panel), followed by reprobe with the anti-phospho-ERK1/2 antibody (lower top panel).

Figure 2 Differential effects of inhibition of cellular signal transduction on the HF6 cells transformed by *FMS-like receptor tyrosine kinase 3* (*FLT3*) mutants. (**a**) Effect of the retroviral transduction with the dominant negative mutant of signal transducer and activator of transcription 5A (dnSTAT5A) in pMXs-internal ribosomal entry site (IRES)-Kusabira-Orange (KO) on the transformed and parental HF6 cells. Viable cell numbers and KO expression were monitored daily after the transduction, and the averages of ratios of each KO-positive cell number at days 1, 2, 3 and 4 to that at day 1 are shown with s.d. (bars). (**b**) Intracellular flow cytometric analyses of phospho-STAT5 (Y694) on the transformed and parental HF6 cells transduced with dnSTAT5A in pMXs-IRES-KO. The density plots show expression of each intracellular antigen labeled with the Alexa Fluor 647-conjugated anti-phospho-STAT5 (Y694) (upper eight panels) or its isotype control (lower two panels) antibody versus expression of KO. As negative controls, nontransduced and mock-transduced HF6 cells were used, respectively (lower two panels using the isotype control antibody). As references, nontransduced HF6 cells were deprived of interleukin-3 (IL-3) for 8 h (HF6 (IL-3(−))), or stimulated with IL-3 for 15 min after the same deprivation (HF6 (IL-3(+))), and then used (lower two panels using the anti-phospho-STAT5 antibody). KO and Alexa Fluor 647 were detected using the FL2 and FL4 channels of the fluorescence-activated cell sorting (FACS) Calibur, respectively. (**c**) Effect of the various concentrations of mitogen-activated protein kinase (MAPK) kinase (MEK) inhibitor, U0126, on the transformed and the parental HF6 cells. The averages with s.d. (bars) of ratios of viable cell numbers in the presence of each concentration of U0126 to those in the absence of U0126 are shown. (**d**) Western blot analyses of the whole lysates extracted from the transformed HF6 cells treated with U0126. Both groups of transformed HF6 cells were treated with various concentrations (shown above each upper panel) of U0126 for 2 h and then harvested. Both blots were probed with the anti-phospho-extracellular signal-related kinase (ERK)1/2 antibody (each top panel), followed by reprobe with the anti-ERK1/2 antibody (each bottom panel).

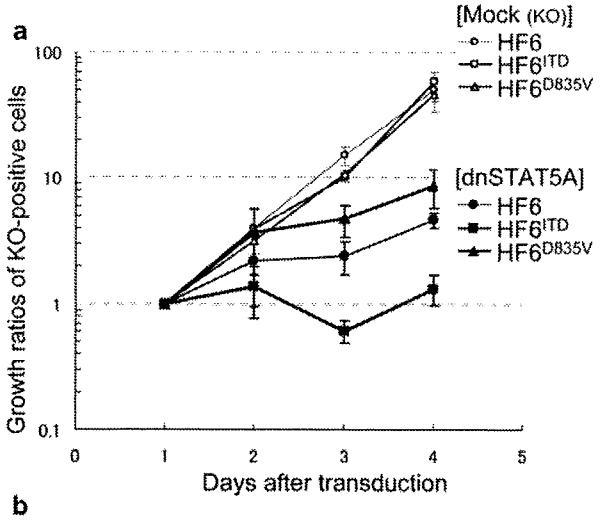
a
[Mock (KO)]
HF6
HF6ITD
HF6D835V
[dnSTAT5A]
HF6
HF6ITD
HF6D835V
Growth ratios of KO-positive cells
Days after transduction

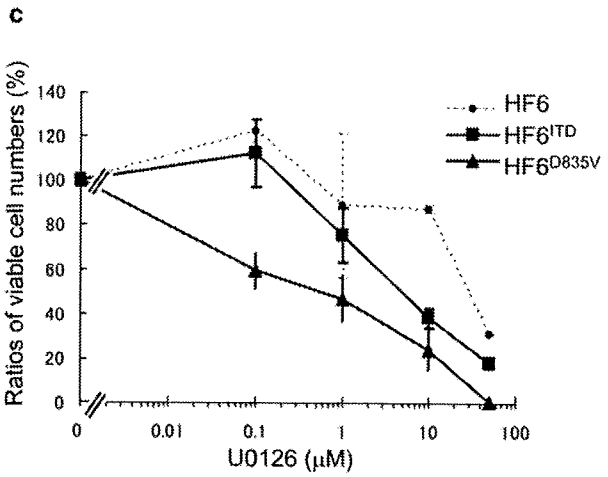
c
HF6
HF6ITD
HF6D835V
Ratios of viable cell numbers (%)
U0126 (μM)

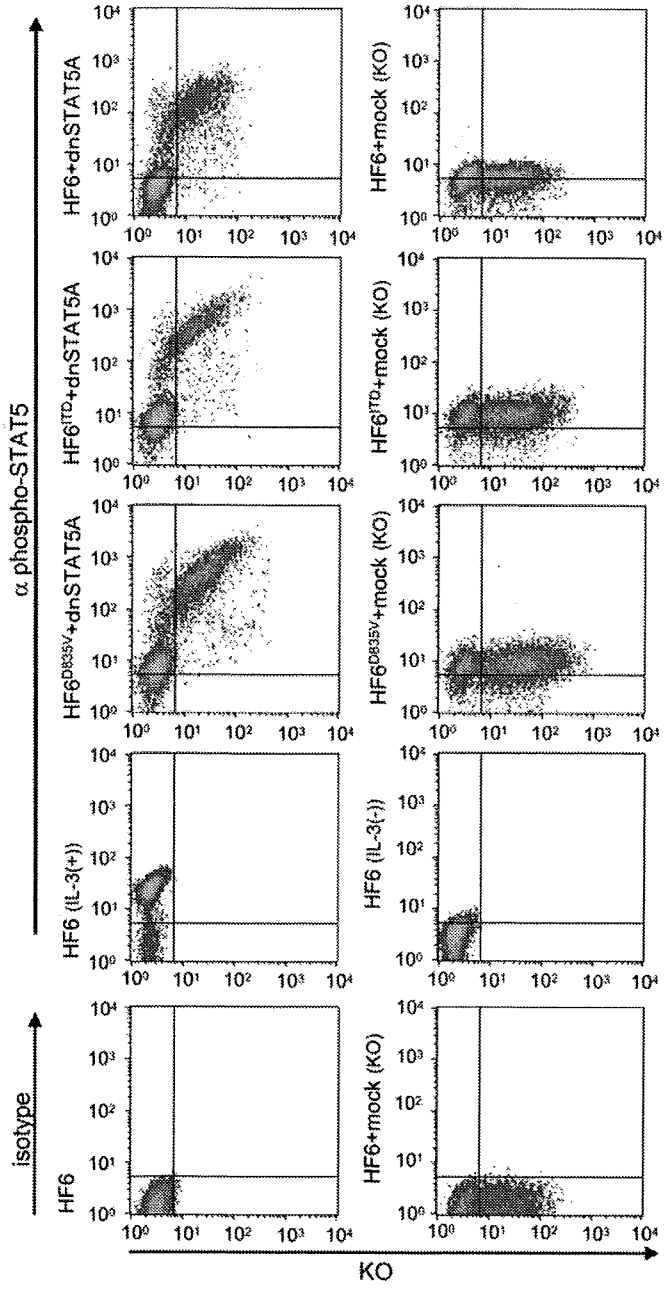
b
HF6+dnSTAT5A
HF6+mock (KO)
HF6ITD+dnSTAT5A
HF6ITD+mock (KO)
HF6D835V+dnSTAT5A
HF6D835V+mock (KO)
HF6 (IL-3(+))
HF6 (IL-3(-))
HF6
HF6+mock (KO)
α phospho-STAT5
isotype
KO

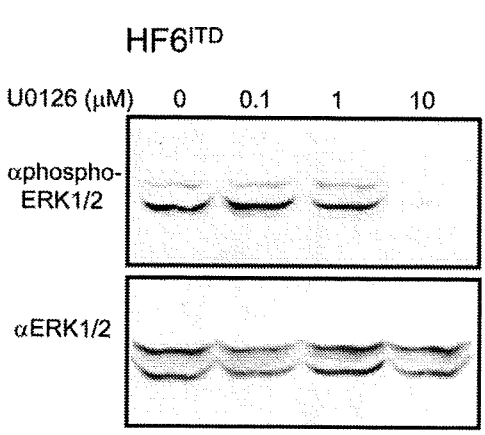
d
HF6ITD
U0126 (μM) 0 0.1 1 10
αphospho-ERK1/2
αERK1/2

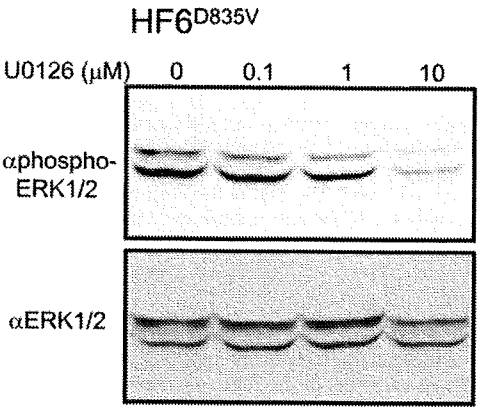
HF6D835V
U0126 (μM) 0 0.1 1 10
αphospho-ERK1/2
αERK1/2

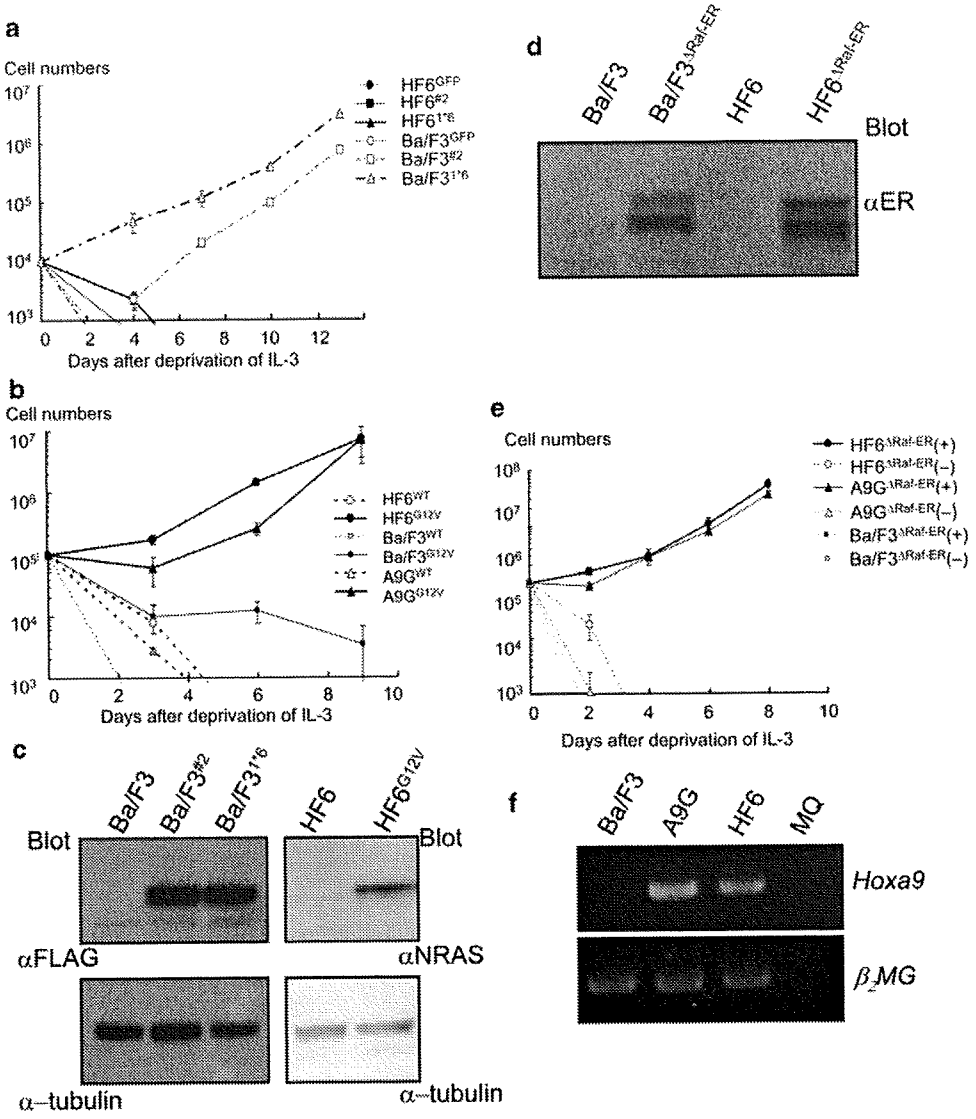

Figure 3 Transformation of the HF6 and A9G cells induced by direct activation of Ras/Raf/mitogen-activated protein kinase (MAPK) pathway. (**a**) Transformation assays of the HF6 and Ba/F3 cells expressing constitutively active forms of signal transducer and activator of transcription 5A (STAT5A) (#2 and 1*6). Green fluorescent protein (GFP) was used as a control. (**b**) Transformation assays of the HF6, A9G and Ba/F3 cells expressing wild-type (WT) *NRAS* or $NRAS^{G12V}$ (G12V). The averages of the number of viable cells with s.d. (bars) are shown in (**a**) and (**b**). (**c**, **d**) Western blot analyses of the whole lysates extracted from the transduced cells (see legends to panels (a) and (b)) in the absence of interleukin-3 (IL-3). (**c**) HF6 and Ba/F3 cells transduced with an inducible form of Raf (Δ*Raf*-estrogen receptor (ER)) (**d**) and their parental cells (**c**, **d**). The blot was probed with the anti-FLAG antibody to detect expression of ectopically expressed STAT5A mutants (upper left panel), or probed with the anti-*NRAS* antibody (upper right panel), followed by reprobe with the anti-α-tubulin antibody as internal control (lower panels) (**c**). The blot was also probed with the anti-ER antibody to detect expression of Δ*Raf*-ER (**d**). (**e**) Transformation assays of the HF6, A9G and Ba/F3 cells expressing Δ*Raf*-ER in the presence of 4-hydroxy-tamoxifen (4-OHT) (+) or vehicle control (−). The averages of the number of viable cells with s.d. (bars) are shown. (**f**) Analysis of *Hoxa9* transcripts in A9G cells using reverse transcriptase-PCR. Ba/F3 and HF6 cells were used as negative and positive controls, respectively.

Figure 4 Leukemogenesis induced by *mixed-lineage-leukemia* (*MLL*)-septin 6 (*SEPT6*) with $NRAS^{G12V}$ synergistically, but not with signal transducer and activator of transcription 5A (STAT5A)#2, *in vivo* under lethal conditioning. (**a**) Survival curves of mice transplanted with *MLL-SEPT6* and $NRAS^{G12V}$ (MS6/G12V; $n=6$), MS6 and *STAT5A*#2 (MS6/#2; $n=6$), MS6/GFP ($n=6$), neo/G12V ($n=6$), neo/#2 ($n=3$) and neo/GFP ($n=3$). (**b**) Representative macroscopic images of spleens obtained from each group of mice shown in (**a**). Scale bar 1 cm. (**c**, **d**) Representative histopathological analysis of morbid mice transplanted with MS6/#2, MS6/G12V (**c**, **d**), neo/G12V, and neo/#2 (**d**). Bone marrow (BM) cells (**c**) and paraffin sections of spleen (**d**) were stained with Wright-Giemsa and hematoxylin and eosin (H&E), respectively. Original magnification, ×200 (**c**) and ×40 (**d**); scale bars, 30 μm (c) and 200 μm (**d**). (**e**, **f**) Immunophenotype of BM or splenic (Sp) cells obtained from representative morbid mice transplanted with MS6/#2 (**e**, left panels), MS6/G12V (**e**, right panels), neo/G12V (**f**, left panels) and neo/#2 (**f**, right panels). The dot plots show each surface antigen labeled with a corresponding monoclonal antibody versus expression of GFP. Ly5.1, Gr-1, CD11b, Ter119, and c-Kit were labeled with phycoerythrin (PE)-conjugated and allophycocyanin (APC)-conjugated monoclonal antibodies, respectively. (**g**) Southern blot analysis to detect clonality (left panel) and proviral integration (right panel). Genomic DNA extracted from BM cells obtained from representative mice transplanted with MS6/G12V (lanes 4, 5, 9 and 10), MS6/GFP (lanes 2, 3, 7 and 8) and neo/GFP (5 months after transplantation; lanes 1 and 6) was digested with *Bam*HI (lanes 1–5) and *Nhe*I (lanes 6–10), respectively, and hybridized with the Neo probe. Oligoclonal bands of proviral integration and single bands of the proviral DNA are indicated by arrows and arrowheads, respectively.

($A9G^{\Delta Raf-ER}$) cells grew without IL-3 only in the presence of 4-hydroxy-tamoxifen (Figure 3e). Expression level of *Hoxa9* in A9G cells was shown in comparison with those in Ba/F3 and HF6 (negative and positive controls, respectively) cells by reverse transcriptase-PCR (Figure 3f).

Taken together, these results *in vitro* suggested the essential role of activation of the Ras/Raf/MAPK cascade together with *Hoxa9* upregulated by *MLL* fusion proteins in the transformation of the cells expressing *MLL* fusion protein.

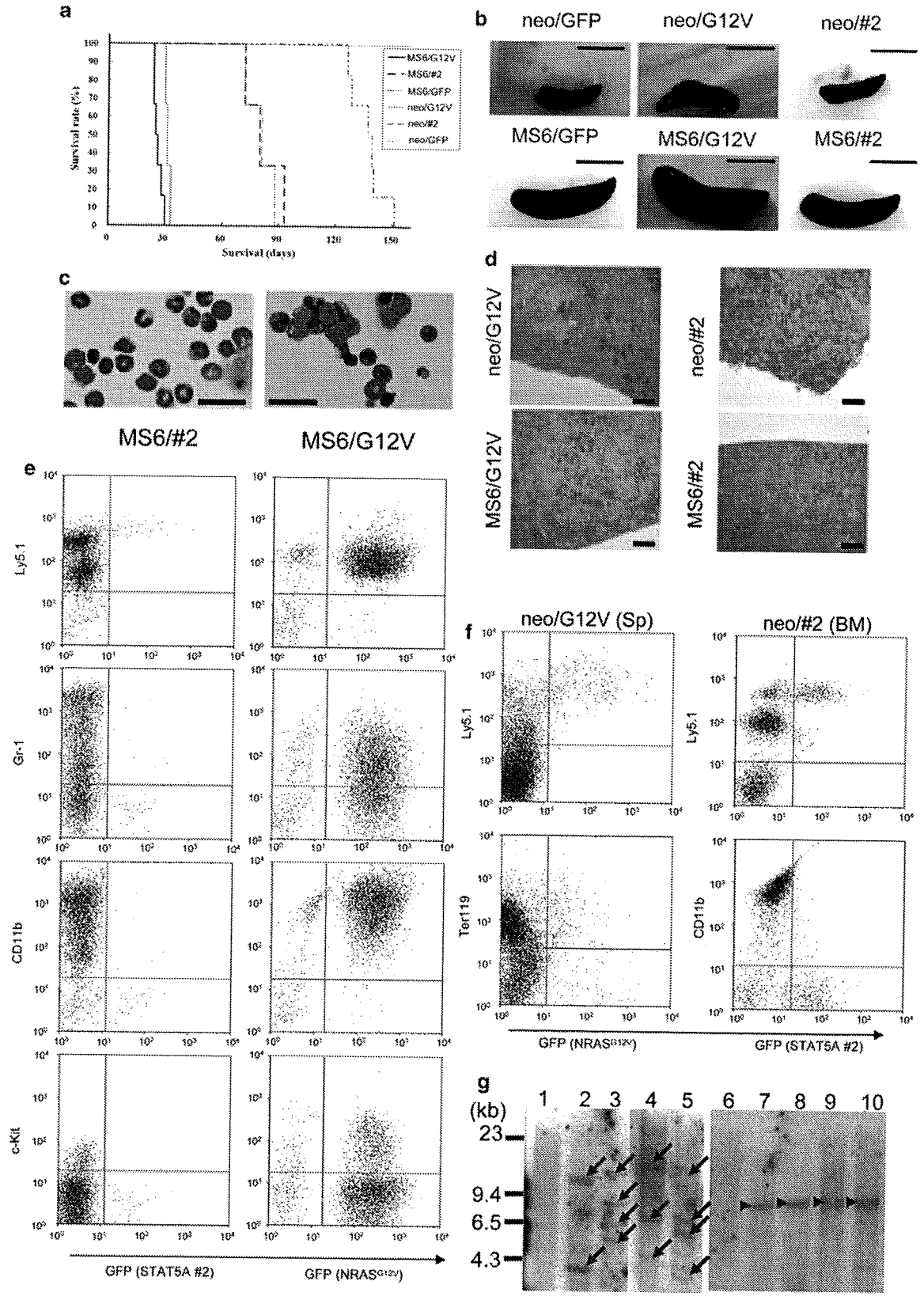

MLL *fusion proteins and oncogenic* NRAS *cooperate to induce acute leukemia, at least partly through aberrant expression of* Hoxa9

The findings on the transformation of HF6 cells *in vitro* led to the hypothesis that *MLL* fusion proteins might cooperate with activation of Ras to induce *AML in vivo*. To test this hypothesis, the oncogenic potential of $NRAS^{G12V}$ (G12V) or STAT5A#2 (#2) to cooperate with *MLL-SEPT6* (MS6) or *MLL-ENL* short form was examined in the leukemogenesis assays *in vivo* (Supplementary Figure 1). STAT5A1*6 was not used owing to its too strong oncogenic potential *in vivo* as reported earlier.[36] The transduction efficiencies of $NRAS^{G12V}$, STAT5A#2 and *MLL-ENL* were 30–50, 20–40 and 5–10%, respectively, as determined by GFP expression (data not shown).

The mice receiving the BM cells transduced with *MLL-SEPT6* and $NRAS^{G12V}$ (MS6/G12V) died with significantly shorter latencies (26 ± 2.4 days; $P<0.05$, log-rank test) than the MS6/GFP mice that died of MPD (137 ± 9.0 days) as described earlier,[6] but, unexpectedly, the neo/G12V mice died as early as the MS6/G12V mice (31 ± 1.4 days) (Figure 4a, Table 1, and data not shown). The MS6/#2 mice died with significantly shorter latencies (82 ± 11 days; $P<0.05$, log-rank test) than the MS6/GFP mice, but as early as the neo/#2 mice (80 ± 8.0 days) (Figure 4a and Table 1). Notably, the phenotypes of the MS6/G12V mice were very different from those of the neo/G12V mice and from MPD in the MS6/GFP mice, whereas those of the MS6/#2 mice were rather similar to MPD in the MS6/GFP mice than those of the neo/#2 mice.

The morbid MS6/G12V mice showed hepatosplenomegaly with various ranges of leukocytosis, anemia and thrombocytopenia, whereas the morbid neo/G12V mice showed no hepatomegaly but mild splenomegaly, and severe pancytopenia (Figure 4b and Table 1). Histopathological analyses of the morbid MS6/G12V mice showed that immature myelomonocytic blasts accounted for more than 30% of BM cells, and severely infiltrated the spleen and the liver (Figures 4c and d, and data not shown). Immunophenotyping analyses of the BM cells also revealed that a majority of these cells expressed GFP, which indicated expression of $NRAS^{G12V}$, with high level of CD11b, intermediate level of Gr-1 (a myeloid differentiation marker also known as Ly-6G) and low level of c-Kit (CD117, the receptor of stem cell factor) (Figure 4e). In addition, Southern blot analysis of genomic DNAs derived from the spleens of the MS6/G12V mice showed oligoclonal bands of proviral integration (Figure 4g). These results indicated that the MS6/G12V mice developed *AML* similar to the mice receiving BM cells transduced with *MLL-SEPT6* and *FLT3*-ITD, as described earlier.[6] In contrast, the morbid neo/G12V mice showed extremely hypocellular marrows and extramedullary hematopoiesis in the spleen, where a majority of the cells did not express Ly5.1 (Figure 4f), with little expression of *Hoxa9* in comparison with the morbid MS6/G12V mice (Supplementary Figure 3a). Thus, this finding suggested that, in our leukemogenesis assays under lethal conditioning, *NRAS* might develop BM aplasia presumably due to engraftment failure. Meanwhile, the MS6/#2 mice died of MPD, showing myeloid hyperplasia consisting predominantly of mature granulocytic elements in the BM cells, where a very small population (1.0%) expressed STAT5A#2, with splenomegaly similar to the MS6/GFP mice (Figures 4b–d, and Table 1). The neo/#2 mice showed neither hepatosplenomegaly nor hematological abnormalities in the peripheral blood, but relative myeloid hyperplasia in the BM, where only a small population (9.4%) expressed STAT5A#2 (Figures 4b and f, data not shown and Table 1), thus implying that STAT5A#2 might induce lethal BM abnormality owing to paracrine expression of some cytokines as in the earlier report using STAT5A1*6.[36]

To generalize leukemogenic cooperation between *MLL* fusion proteins and oncogenic *NRAS* and avoid the early death caused by transduction of $NRAS^{G12V}$, the BM cells transduced with *MLL-ENL* and/or oncogenic *NRAS* were also transplanted into recipient mice under sublethal conditioning. The *MLL-ENL* short form was used for leukemogenesis assays under sublethal conditioning with oncogenic *NRAS* ($NRAS^{G12V}$), in which retroviral vectors were exchanged, so that the expression of GFP indicated that of *MLL-ENL* (Supplementary Figure 1). These leukemogenesis assays under sublethal conditioning confirmed that the combination of *MLL-ENL* and $NRAS^{G12V}$ reproduced *AML*, and that *MLL-ENL* (and puro) induced the phenotype of MPD (Figures 5a, b and d, and Table 1). Meanwhile, $NRAS^{G12V}$

Table 1 Characteristics of the morbid mice transplanted with hematopoietic progenitors transduced with *MLL* fusion genes or *Hoxa9*, and/or either $NRAS^{G12V}$ or STAT5A #2

Mouse	*Latency (days)*	*Liver (g)*	*Spleen (g)*	*Thymus (g)*	*WBC (per μl)*	*Hb (g per 100 ml)*	*Plt (× 10^4 per μl)*
Lethal conditioning							
MS6/G12V ($n=6$)	26 ± 2.4	1.60 ± 0.35	0.31 ± 0.07	0.020 ± 0.012	74 600 ± 62 900	4.2 ± 1.0	4.0 ± 3.9
MS6/#2 ($n=3$)[a]	82 ± 11	0.98 ± 0.43	0.32 ± 0.03	0.019 ± 0.006	73 100	5.3	4.4
MS6/GFP ($n=6$)	137 ± 9.0	1.54 ± 0.69	0.26 ± 0.09	0.037 ± 0.005	309 000 ± 263 000	7.0 ± 6.6	8.0 ± 5.7
neo/G12V ($n=6$)	31 ± 1.4	1.04 ± 0.25	0.25 ± 0.08	0.030 ± 0.030	4600 ± 1800	2.5 ± 0.3	0.5 ± 0.4
neo/#2 ($n=3$)[a]	80 ± 8.0	0.66 ± 0.16	0.08 ± 0.06	0.011 ± 0.001	9800	18.8	58.2
neo/GFP ($n=3$)	NA	1.36 ± 0.11	0.09 ± 0.01	0.051 ± 0.010	12 000 ± 4700	14.7 ± 0.6	81 ± 13
A9/G12V ($n=4$)	28 ± 7.5	1.93 ± 0.56	0.44 ± 0.16	0.033 ± 0.030	76 300 ± 56 700	4.5 ± 2.7	1.0 ± 0.6
A9/GFP ($n=6$)	NA	NT	NT	NT	21 200 ± 5400	17.3 ± 2.4	66 ± 4.7
puro/GFP ($n=3$)	NA	1.48 ± 0.21	0.06 ± 0.01	0.049 ± 0.022	12 000 ± 3400	13.6 ± 1.5	81 ± 19
Sublethal conditioning							
MEs/G12V ($n=10$)	21 ± 3.9	2.56 ± 0.45	0.51 ± 0.10	0.043 ± 0.020	164 000 ± 131 000	7.2 ± 2.5	11 ± 4.5
MEs/puro ($n=5$)	89 ± 11	1.89 ± 0.58	0.44 ± 0.11	0.043 ± 0.006	99 000 ± 53 000	7.4 ± 2.9	9.1 ± 3.1
GFP/G12V ($n=5$)[b]	89 ± 10	0.90 ± 0.31	0.06 ± 0.03	0.63 ± 0.35	22 000 ± 1000	13.6 ± 1.7	97
GFP/puro ($n=3$)	NA	NT	NT	NT	NT	NT	NT

Abbreviations: GFP, green fluorescent protein; Hb, hemoglobin; MEs, *MLL-ENL* short form; NA, not applicable; NT, not tested; Plt, platelet; WBC, white blood cell.
Averages with s.d. are shown.
[a]Blood cell counts of only one morbid mouse were performed.
[b]One mouse developing acute leukemia and thymoma was excluded, owing to the remarkably increased number of WBCs and hepatosplenomegaly. The platelet count of only one morbid mouse was determined.

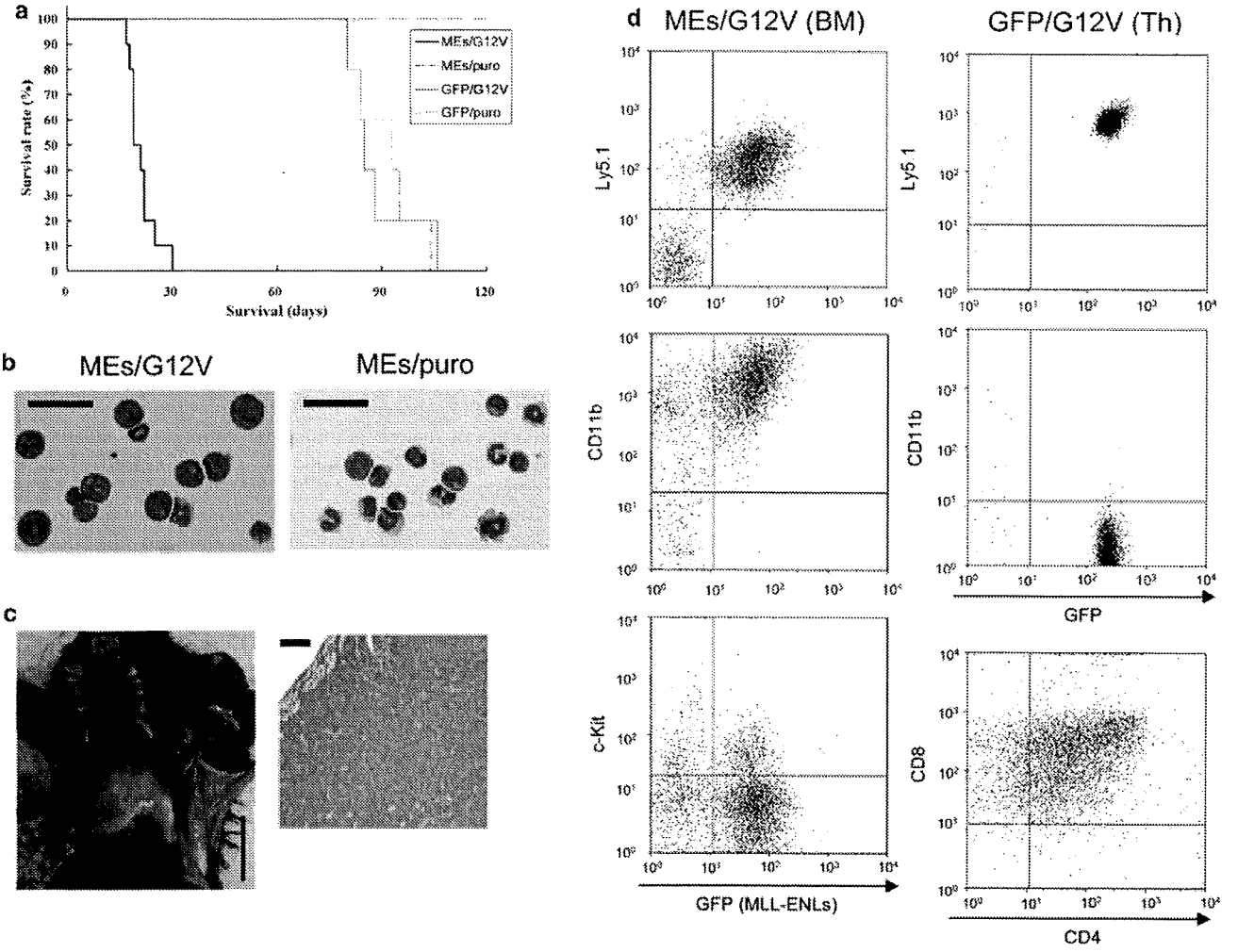

Figure 5 Leukemogenesis assays under sublethal conditioning using *mixed-lineage-leukemia/eleven nineteen leukemia* (*MLL-ENL*) and $NRAS^{G12V}$. (**a**) Survival curves of mice transplanted with a short form of *MLL-ENL* (MEs) and $NRAS^{G12V}$ (MEs/G12V) ($n=10$), MEs/puro ($n=5$), GFP/G12V ($n=5$) and green fluorescent protein (GFP)/puro ($n=3$). (**b**) Representative cytospin preparations of bone marrow (BM) cells obtained from morbid MEs/G12V and MEs/puro mice. The cells were stained with Wright-Giemsa. Original magnification 200×; Scale bars 30 μm. (**c**) Representative histopathologic images of thymus obtained from the GFP/G12V mouse. A paraffin section of the thymus was stained with hematoxylin and eosin (H&E). Original magnification, ×40; vertical and horizontal scale bars, 1 cm and 200 μm, respectively. (**d**) Immunophenotype of BM and thymic (Th) cells obtained from representative morbid MEs/G12V and GFP/G12V mice. The dot plots show each surface antigen labeled with a corresponding monoclonal antibody versus expression of GFP or CD4. Ly5.1, CD11b, CD4, and c-Kit and CD8 were labeled with phycoerythrin (PE)-conjugated and allophycocyanin (APC)-conjugated monoclonal antibodies, respectively.

(and GFP) led to thymoma, sometimes together with leukocytosis, with a long latency (Figures 5a, c and d, and Table 1). In addition, to examine the possibility that the phenotypes associated with STAT5A#2 might change, similar to oncogenic *NRAS*, the BM cells transduced with STAT5A#2 (in pMYs-IRES-EGFP) and/or *MLL-SEPT6* (in pMXs-neo) were again transplanted into recipient mice under sublethal conditioning. Within an observation period of 160 days, two of three neo/#2 mice under sublethal conditioning died with longer latencies (134 and 139 days) and showed the same phenotype of myeloid hyperplasia in the BM, where a small population (15%) expressed STAT5A#2, although these had different phenotypes of pancytopenia and splenomegaly (Supplementary Figure 3b and data not shown). In contrast, two of three MS6/#2 mice and all of the three MS6/GFP mice survived and showed no hematological abnormalities in the peripheral blood, whereas one of the MS6/#2 mice died (125 day) but could not be analyzed because of post-mortem change, within the observation period. Histopathological analysis of one MS6/#2 mouse, which was killed 150 days after the transplantation, showed no significant hepatosplenomegaly but mild myeloid hyperplasia in the BM (data not shown). Only 30% of the BM cells were positive for donor-derived Ly-5.1, and 7% of the BM cells were positive for GFP, indicating expression of STAT5A#2 (Supplementary Figure 3c), whereas reverse transcriptase-PCR analysis of the BM cells gave very weak signals of *MLL-SEPT6* after 30 cycles (data not shown), but clearly visible signals after 35 cycles (Supplementary Figure 3c). Therefore, sublethal conditioning seemed to be inappropriate for leukemogenesis assays using oncogenes, such as *MLL-SEPT6* and STAT5A#2, which had relatively weak oncogenic potential in comparison with *MLL-ENL* and $NRAS^{G12V}$.

Finally, we examined whether *Hoxa9* may be involved in cooperation between the *MLL* fusion protein and oncogenic *NRAS in vivo*, such as in transformation assays *in vitro*. The leukemogenesis assays using the BM cells transduced with

Hoxa9 and oncogenic *NRAS* were carried out under lethal conditioning, because preliminary leukemogenesis assays under sublethal conditioning were unsuccessful probably because of engraftment failure (data not shown). The combination of *Hoxa9* and $NRAS^{G12V}$ (A9/G12V) led to death with short latencies (28 ± 7.5 days) (Figure 6a and Table 1), whereas *Hoxa9* (and GFP) *per se* induced no lethal disease within 120 days, as reported earlier.[37] The A9/G12V mice showed remarkable hepatosplenomegaly and had a tendency toward leukocytosis, anemia and thrombocytopenia (Table 1). Histopathological and immunophenotyping analyses of the BM cells revealed that the A9/G12V mice had a few, but prominent, myelomonocytic blasts (Figure 6b), with high expression of CD11b and Gr-1, and low level of c-Kit (Figure 6c). A Southern blot analysis of genomic DNAs derived from the spleens of the A9/G12V mice gave oligoclonal bands (data not shown). These results indicated that *Hoxa9* cooperated with oncogenic *NRAS* to rapidly induce lethal myeloid malignancy that was not identical but similar to the acute leukemia induced by *MLL* fusion proteins and oncogenic *NRAS*.

Taken together, these results *in vivo* suggested that *MLL* fusion proteins rapidly induce acute leukemia together with activated *NRAS*, at least in part through aberrant expression of *Hoxa9*.

Discussion

The present study provides several evidences that *MLL*-fusion-mediated leukemogenesis cooperated synergistically with Ras activation, but not with STAT5 activation. Although all known *MLL* fusion proteins were not tested in this study, we showed that this synergistic cooperation was not limited to the specific *MLL* fusion, using two different well-characterized types of *MLL* fusion proteins. In the light of the role of FLT3 mutations in *MLL*-fusion-mediated leukemogenesis described earlier,[6] signaling pathways downstream of FLT3 mutations were analyzed in the transfectants of HF6, a cell line expressing *MLL-SEPT6*. The immortalized cells, such as HF6 and A9G, used in this study might have acquired additional mutations. However, the phenotypes including IL-3 dependency, expression patterns of lineage markers and growth rates were not changed since their establishment (data not shown), thus suggesting that at least no mutations leading to critical transformation had occurred in these cell lines. Although recent studies have disclosed the differences in activation of signal molecules, including MAPK and STAT5, between *FLT3*-TKD and *FLT3*-ITD,[24,38] our experiments using transduction with FLT3 mutants and inhibition of the signal molecules first showed a crucial role of activation of MAPK rather than STAT5 in the factor-independent survival and proliferation of HF6 cells. Next, the myeloid transformation assays *in vitro* revealed that the activation of Raf-1, as well as oncogenic *NRAS*, transformed HF6 cells, but that constitutively active mutants (1*6 and #2) of STAT5A did not. The leukemogenesis assays *in vivo* also showed that oncogenic *NRAS* rapidly induced acute leukemia together with *MLL* fusion proteins, which differed from the original phenotype induced by each molecule. In contrast, the active STAT5A mutant did not confer obvious synergistic effects on the *MLL*-fusion-mediated leukemogenesis. Thus, these results *in vitro* and *in vivo* suggested that activation of the Ras/Raf/MAPK pathway may be sufficient for the transformation of HF6 cells and development of *MLL*-fusion-mediated leukemia.

Oncogenic *NRAS* induced thymoma in the leukemogenesis assays under sublethal conditioning, which is consistent with the

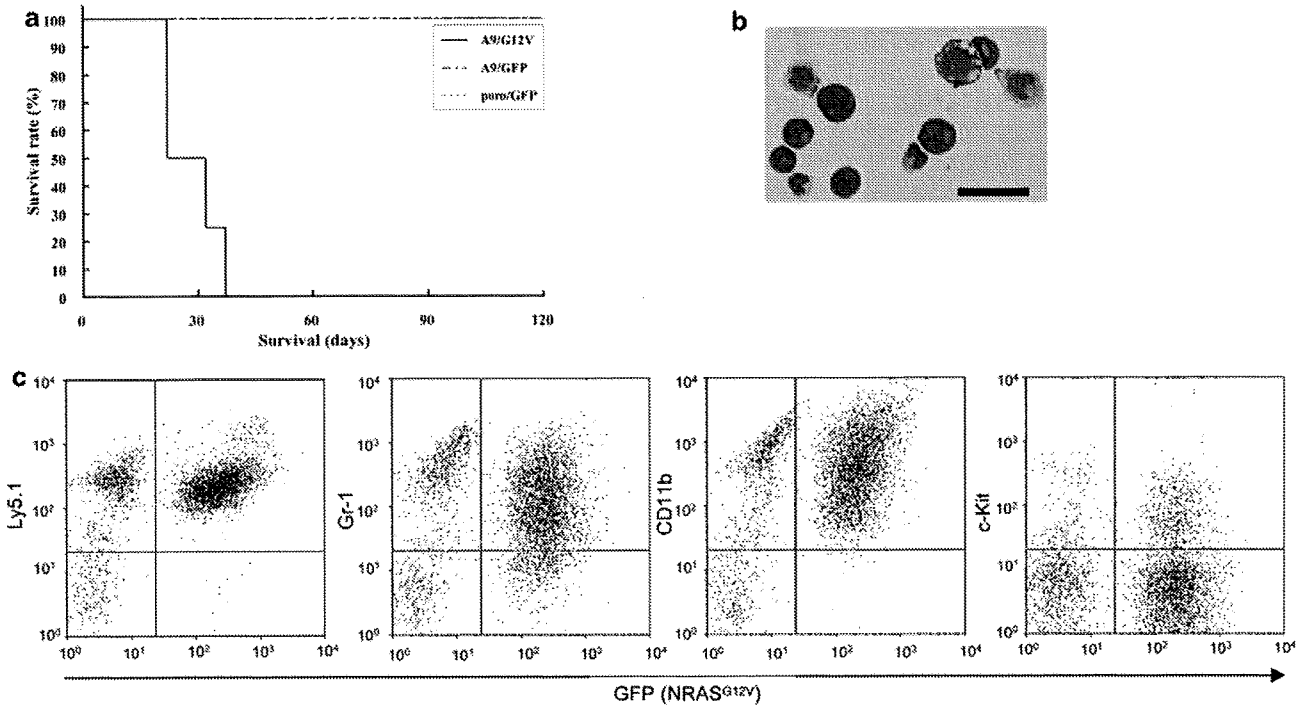

Figure 6 Leukemogenesis induced by *Hoxa9* and oncogenic neuroblastoma RAS viral (v-ras) oncogene homolog (*NRAS*) under lethal conditioning. (**a**) Survival curves of mice transplanted with *Hoxa9* and $NRAS^{G12V}$ (A9/G12V; $n=4$), A9/green fluorescent protein (GFP) ($n=6$) and puro/GFP ($n=3$). (**b**) Representative cytospin preparations of bone marrow (BM) cells obtained from morbid A9/G12V mice. The cells were stained with Wright-Giemsa. Original magnification, × 200; scale bar, 30 μm. (**c**) Immunophenotype of BM cells obtained from representative morbid A9/G12V mice. The dot plots show each surface antigen labeled with a corresponding monoclonal antibody versus expression of GFP. Ly5.1, Gr-1, CD11b, and c-Kit were labeled with phycoerythrin (PE)-conjugated and allophycocyanin (APC)-conjugated monoclonal antibodies, respectively.

development of T-lymphoma by *FLT3*-TKD in our experimental system (Ono *et al.*, unpublished data), whereas it led to the development of BM aplasia in our leukemogenesis assays under lethal conditioning. This difference in the disease phenotypes implies that forced expression of oncogenic *NRAS* in BM progenitors might be involved in its inhibitory effects on the engraftment of radioprotective cells as well as the antiproliferative effect of oncogenic *NRAS* in the early phase of the transplantation.[39] These disease phenotypes were also different from the development of MPD in the earlier reports.[39,40] This discrepancy might be due to the differences in the experimental systems, such as the retroviral transduction and mice strains. Meanwhile, the BM progenitors transduced with *Hoxa9* and $NRAS^{G12V}$ seemed to result in engraftment failure under sublethal conditioning, but these rapidly developed myeloid malignancy under lethal conditioning. A recent study using BM transplantation showed the possibility of drastic fluctuation in the engraftment of donor cells receiving pathological modification under sublethal conditioning;[41] hence, our unsuccessful results under sublethal conditioning might be associated with some instability of the transplantation.

Our leukemogenesis assays showed a definitively synergistic cooperation between *MLL* fusion proteins and oncogenic *NRAS* in the acceleration of disease onset and change of the phenotypes. Interestingly, the synergistic cooperation between *MLL* fusion proteins and Ras/Raf/MAPK activation closely correlated with recent clinical studies reporting the frequent coincidence of *MLL* fusion genes and mutations of *RAS*[20] or *RAF*.[42] It was reported that the additional expression of oncogenic *KRAS* induced an acute promyelocytic leukemia-like disease in transgenic mice expressing promyelocytic leukemia/retinoic acid receptor-α with an increased penetrance and decreased latency, although neither the penetrance nor the latency was significantly different from those in mice that died of MPD by expression of oncogenic *KRAS* alone.[43] Other groups recently reported that the combination of oncogenic *NRAS* and *MLL-AF9*[44] or *MLL-ENL*[45] is capable of developing *AML*, and that induced repression of oncogenic *NRAS* on the combination reverted *AML* to MPD by the *MLL* fusion gene (*MLL-AF9*) alone.[44] Although our findings that *MLL* fusion proteins and oncogenic *NRAS* cooperate to induce *AML* confirmed these notions, the present study further analyzed the involvement of *Hoxa9* and Raf, downstream of the cooperation between *MLL* fusion proteins and oncogenic *NRAS*. The myeloid transformation assays *in vitro* showed that the activation of Raf-1, as well as oncogenic *NRAS*, transformed A9G, a cell line expressing *Hoxa9*. The leukemogenesis assays *in vivo* also showed that *Hoxa9* and oncogenic *NRAS* rapidly developed myeloid malignancy. These results *in vitro* and *in vivo* suggested that, as downstream molecules, *Hoxa9* and Raf may have important roles in the synergistic leukemogenesis by *MLL* fusion proteins and oncogenic *NRAS*.

Our findings suggest a possible model of *MLL*-fusion-mediated leukemogenesis that was essentially recapitulated by *Hoxa9* expression and Ras/Raf/MAPK activation (Figure 7). In the context of secondary genetic alterations, such as *FLT3* mutations, this model explains the clinical features of acute leukemia with 11q23 translocations. First, overexpression, as well as TKD mutations, of *FLT3* frequently detected in the *MLL*-rearranged infant acute leukemia may be involved in the leukemogenesis mainly through activation of Ras/Raf/MAPK, because several studies reported that the signaling pathway of wild-type *FLT3* is similar to *FLT3*-TKD rather than *FLT3*-ITD.[24,38] Second, besides *FLT3*, other unknown molecular pathways that lead to the activation of Ras/Raf/MAPK might also be involved in

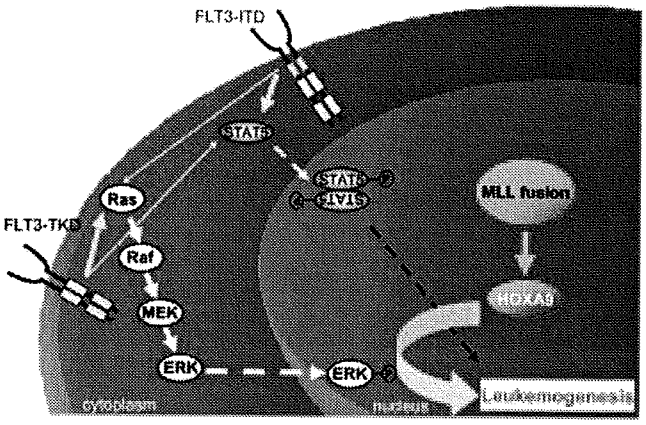

Figure 7 A model of *mixed-lineage-leukemia* (*MLL*)-mediated leukemogenesis together with secondary genetic alterations. *MLL* fusion protein and secondary genetic alterations cooperate to induce acute leukemia through synergistic molecular crosstalk between aberrant expression of *Hox* genes, including *Hoxa9*, and the activation of Ras/Raf/mitogen-activated protein kinase (MAPK). Other signaling pathways, including signal transducer and activator of transcription 5 (STAT5) activation, only additively affect the leukemogenic potential.

the *MLL*-rearranged leukemia carrying no known genetic alterations, as *FLT3* alterations are not found very frequently in most *MLL*-rearranged leukemia except in infants.[46,47] Meanwhile, in the context of *MLL* fusion proteins, we analyzed the role of the *Hoxa9*-mediated pathway leading to leukemogenesis. Recent studies revealed that one of the *Hox*-cofactor molecules, *Meis1*, is an essential molecule involved in normal hematopoiesis[48] as well as *Hoxa9*-mediated leukemogenesis.[49] However, our experimental system[6] using BM cells transduced with *MLL* fusion proteins did not detect any significant upregulation of *Meis1* in comparison with the mock transduction as reported earlier,[50] in contrast with the findings by other groups.[14] Therefore, we focused on *Hoxa9*, one of the key molecules directly upregulated by *MLL* fusion proteins. Interestingly, a recent study showed that the combination of *Hoxa9* and *Meis1* cooperated with *Trib1*, which enhanced the phosphorylation of ERK, to induce acute leukemia in the BM transplantation assays.[51] Their study is not inconsistent with our findings; thus, the *HOX* and Ras/Raf/MAPK axes may have central roles in the molecular network of *MLL*-mediated leukemogenesis, which might be additively affected by other pathways, such as activation of STAT5 (Figure 7). In addition, at least, endogenous expression of *Meis1* in A9G cells is also considered to be important in this network, but further analysis will be required to clarify the role of *Meis1* in the collaboration between *HOX* and MAPK axes.

Conclusion

This study suggests that *MLL* fusion proteins synergistically cooperate with Ras/Raf/MAPK activation in leukemogenesis, at least partly through the upregulation of *Hoxa9*. Future studies analyzing the molecular crosstalk between *Hoxa9* and the Ras/Raf/MAPK cascade are expected to provide novel insights into the molecular mechanism of *MLL*-fusion-mediated leukemogenesis.

Conflict of interest

The authors declare no conflict of interest.

Acknowledgements

We thank Dr Guy Sauvageau (Laboratory of Molecular Genetics of Stem Cells, Institute for Research in Immunology and Cancer, Canada) for the plasmid harboring a fragment of *Hoxa9*, and Dr Yusuke Satoh (Hematology and Oncology, Osaka University Graduate School of Medicine, Osaka, Japan) for technical advice. We are also grateful to R&D Systems for providing cytokines, and Brian Quinn for language assistance. This work was supported in part by Chugai Pharmaceutical Company Ltd, Grants-in-Aid from the Ministry of Education, Culture, Sports, Science, and Technology in Japan, the Novartis Foundation (Japan) for the Promotion of Science and the Japan Leukaemia Research Fund.

References

1 Vogelstein B, Kinzler KW. Cancer genes and the pathways they control. *Nat Med* 2004; **10**: 789–799.
2 Look AT. Oncogenic transcription factors in the human acute leukemias. *Science* 1997; **278**: 1059–1064.
3 Rowley JD. The critical role of chromosome translocations in human leukemias. *Annu Rev Genet* 1998; **32**: 495–519.
4 Gilliland DG, Tallman MS. Focus on acute leukemias. *Cancer Cell* 2002; **1**: 417–420.
5 Kelly LM, Kutok JL, Williams IR, Boulton CL, Amaral SM, Curley DP *et al.* PML/RARalpha and FLT3-ITD induce an APL-like disease in a mouse model. *Proc Natl Acad Sci USA* 2002; **99**: 8283–8288.
6 Ono R, Nakajima H, Ozaki K, Kumagai H, Kawashima T, Taki T *et al.* Dimerization of MLL fusion proteins and FLT3 activation synergize to induce multiple-lineage leukemogenesis. *J Clin Invest* 2005; **115**: 919–929.
7 Schessl C, Rawat VP, Cusan M, Deshpande A, Kohl TM, Rosten PM *et al.* The *AML1-ETO* fusion gene and the FLT3 length mutation collaborate in inducing acute leukemia in mice. *J Clin Invest* 2005; **115**: 2159–2168.
8 Stubbs MC, Kim YM, Krivtsov AV, Wright RD, Feng Z, Agarwal J *et al.* MLL-AF9 and FLT3 cooperation in acute myelogenous leukemia: development of a model for rapid therapeutic assessment. *Leukemia* 2008; **22**: 66–77.
9 Watanabe-Okochi N, Kitaura J, Ono R, Harada H, Harada Y, Komeno Y *et al.* AML1 mutations induced MDS and MDS/AML in a mouse BMT model. *Blood* 2008; **111**: 4297–4308.
10 Ayton PM, Cleary ML. Molecular mechanisms of leukemogenesis mediated by MLL fusion proteins. *Oncogene* 2001; **20**: 5695–5707.
11 Meyer C, Kowarz E, Hofmann J, Renneville A, Zuna J, Trka J *et al.* New insights to the MLL recombinome of acute leukemias. *Leukemia* 2009; **23**: 1490–1499.
12 Yokoyama A, Somervaille TC, Smith KS, Rozenblatt-Rosen O, Meyerson M, Cleary ML. The menin tumor suppressor protein is an essential oncogenic cofactor for MLL-associated leukemogenesis. *Cell* 2005; **123**: 207–218.
13 Daser A, Rabbitts TH. Extending the repertoire of the *mixed-lineage leukemia* gene *MLL* in leukemogenesis. *Genes Dev* 2004; **18**: 965–974.
14 Hess JL. MLL: a histone methyltransferase disrupted in leukemia. *Trends Mol Med* 2004; **10**: 500–507.
15 Corral J, Lavenir I, Impey H, Warren AJ, Forster A, Larson TA *et al.* An *MLL-AF9* fusion gene made by homologous recombination causes acute leukemia in chimeric mice: a method to create fusion oncogenes. *Cell* 1996; **85**: 853–861.
16 Drynan LF, Pannell R, Forster A, Chan NM, Cano F, Daser A *et al.* MLL fusions generated by Cre-loxP-mediated *de novo* translocations can induce lineage reassignment in tumorigenesis. *EMBO J* 2005; **24**: 3136–3146.
17 Wang J, Iwasaki H, Krivtsov A, Febbo PG, Thorner AR, Ernst P *et al.* Conditional *MLL-CBP* targets GMP and models therapy-related myeloproliferative disease. *EMBO J* 2005; **24**: 368–381.
18 Chen W, Li Q, Hudson WA, Kumar A, Kirchhof N, Kersey JH. A murine *MLL-AF4* knock-in model results in lymphoid and myeloid deregulation and hematologic malignancy. *Blood* 2006; **108**: 669–677.
19 Taketani T, Taki T, Sugita K, Furuichi Y, Ishii E, Hanada R *et al.* FLT3 mutations in the activation loop of tyrosine kinase domain are frequently found in infant ALL with *MLL* rearrangements and pediatric ALL with hyperdiploidy. *Blood* 2004; **103**: 1085–1088.
20 Liang DC, Shih LY, Fu JF, Li HY, Wang HI, Hung IJ *et al.* K-Ras mutations and N-Ras mutations in childhood acute leukemias with or without mixed-lineage leukemia gene rearrangements. *Cancer* 2006; **106**: 950–956.
21 Gilliland DG, Griffin JD. The roles of FLT3 in hematopoiesis and leukemia. *Blood* 2002; **100**: 1532–1542.
22 Armstrong SA, Staunton JE, Silverman LB, Pieters R, den Boer ML, Minden MD *et al.* *MLL* translocations specify a distinct gene expression profile that distinguishes a unique leukemia. *Nat Genet* 2002; **30**: 41–47.
23 Murata K, Kumagai H, Kawashima T, Tamitsu K, Irie M, Nakajima H *et al.* Selective cytotoxic mechanism of GTP-14564, a novel tyrosine kinase inhibitor in leukemia cells expressing a constitutively active Fms-like tyrosine kinase 3 (FLT3). *J Biol Chem* 2003; **278**: 32892–32898.
24 Choudhary C, Schwable J, Brandts C, Tickenbrock L, Sargin B, Kindler T *et al.* AML-associated Flt3 kinase domain mutations show signal transduction differences compared with Flt3 ITD mutations. *Blood* 2005; **106**: 265–273.
25 Nosaka T, Kawashima T, Misawa K, Ikuta K, Mui AL, Kitamura T. STAT5 as a molecular regulator of proliferation, differentiation and apoptosis in hematopoietic cells. *EMBO J* 1999; **18**: 4754–4765.
26 Schubbert S, Shannon K, Bollag G. Hyperactive Ras in developmental disorders and cancer. *Nat Rev Cancer* 2007; **7**: 295–308.
27 Ariyoshi K, Nosaka T, Yamada K, Onishi M, Oka Y, Miyajima A *et al.* Constitutive activation of STAT5 by a point mutation in the SH2 domain. *J Biol Chem* 2000; **275**: 24407–24413.
28 Onishi M, Nosaka T, Misawa K, Mui AL, Gorman D, McMahon M *et al.* Identification and characterization of a constitutively active STAT5 mutant that promotes cell proliferation. *Mol Cell Biol* 1998; **18**: 3871–3879.
29 Kitamura T, Koshino Y, Shibata F, Oki T, Nakajima H, Nosaka T *et al.* Retrovirus-mediated gene transfer and expression cloning: powerful tools in functional genomics. *Exp Hematol* 2003; **31**: 1007–1014.
30 Kroon E, Krosl J, Thorsteinsdottir U, Baban S, Buchberg AM, Sauvageau G. Hoxa9 transforms primary bone marrow cells through specific collaboration with Meis1a but not Pbx1b. *EMBO J* 1998; **17**: 3714–3725.
31 Sakaue-Sawano A, Kurokawa H, Morimura T, Hanyu A, Hama H, Osawa H *et al.* Visualizing spatiotemporal dynamics of multicellular cell-cycle progression. *Cell* 2008; **132**: 487–498.
32 Calvo KR, Sykes DB, Pasillas M, Kamps MP. Hoxa9 immortalizes a granulocyte-macrophage colony-stimulating factor-dependent promyelocyte capable of biphenotypic differentiation to neutrophils or macrophages, independent of enforced meis expression. *Mol Cell Biol* 2000; **20**: 3274–3285.
33 Ono R, Ihara M, Nakajima H, Ozaki K, Kataoka-Fujiwara Y, Taki T *et al.* Disruption of *Sept6*, a fusion partner gene of *MLL*, does not affect ontogeny, leukemogenesis induced by *MLL-SEPT6*, or phenotype induced by the loss of *Sept4*. *Mol Cell Biol* 2005; **25**: 10965–10978.
34 Nosaka T, van Deursen JM, Tripp RA, Thierfelder WE, Witthuhn BA, McMickle AP *et al.* Defective lymphoid development in mice lacking Jak3. *Science* 1995; **270**: 800–802.
35 Moriggl R, Gouilleux-Gruart V, Jähne R, Berchtold S, Gartmann C, Liu X *et al.* Deletion of the carboxyl-terminal transactivation domain of MGF-STAT5 results in sustained DNA binding and a dominant negative phenotype. *Mol Cell Biol* 1996; **16**: 5691–5700.
36 Schwaller J, Parganas E, Wang D, Cain D, Aster JC, Williams IR *et al.* STAT5 is essential for the myelo- and lymphoproliferative disease induced by TEL/JAK2. *Mol Cell* 2000; **6**: 693–704.
37 Nakamura T, Largaespada DA, Shaughnessy Jr JD, Jenkins NA, Copeland NG. Cooperative activation of Hoxa and Pbx1-related genes in murine myeloid leukaemias. *Nat Genet* 1996; **12**: 149–153.
38 Grundler R, Miething C, Thiede C, Peschel C, Duyster J. FLT3-ITD and tyrosine kinase domain mutants induce 2 distinct phenotypes in a murine bone marrow transplantation model. *Blood* 2005; **105**: 4792–4799.

39 MacKenzie KL, Dolnikov A, Millington M, Shounan Y, Symonds G. Mutant N-ras induces myeloproliferative disorders and apoptosis in bone marrow repopulated mice. *Blood* 1999; **93**: 2043–2056.
40 Parikh C, Subrahmanyam R, Ren R. Oncogenic NRAS rapidly and efficiently induces CMML- and AML-like diseases in mice. *Blood* 2006; **108**: 2349–2357.
41 Santaguida M, Schepers K, King B, Sabnis AJ, Forsberg EC, Attema JL *et al.* JunB protects against myeloid malignancies by limiting hematopoietic stem cell proliferation and differentiation without affecting self-renewal. *Cancer Cell* 2009; **15**: 341–352.
42 Christiansen DH, Andersen MK, Desta F, Pedersen-Bjergaard J. Mutations of genes in the receptor tyrosine kinase (RTK)/RAS-BRAF signal transduction pathway in therapy-related myelodysplasia and acute myeloid leukemia. *Leukemia* 2005; **19**: 2232–2240.
43 Chan IT, Kutok JL, Williams IR, Cohen S, Moore S, Shigematsu H *et al.* Oncogenic K-ras cooperates with PML-RAR alpha to induce an acute promyelocytic leukemia-like disease. *Blood* 2006; **108**: 1708–1715.
44 Kim WI, Matise I, Diers MD, Largaespada DA. RAS oncogene suppression induces apoptosis followed by more differentiated and less myelosuppressive disease upon relapse of acute myeloid leukemia. *Blood* 2009; **113**: 1086–1096.
45 Zuber J, Radtke I, Pardee TS, Zhao Z, Rappaport AR, Luo W *et al.* Mouse models of human AML accurately predict chemotherapy response. *Genes Dev* 2009; **23**: 877–889.
46 Chillon MC, Fernandez C, Garcia-Sanz R, Balanzategui A, Ramos F, Fernandez-Calvo J *et al.* FLT3-activating mutations are associated with poor prognostic features in AML at diagnosis but they are not an independent prognostic factor. *Hematol J* 2004; **5**: 239–246.
47 Bacher U, Haferlach C, Kern W, Haferlach T, Schnittger S. Prognostic relevance of FLT3-TKD mutations in AML: the combination matters–an analysis of 3082 patients. *Blood* 2008; **111**: 2527–2537.
48 Hisa T, Spence SE, Rachel RA, Fujita M, Nakamura T, Ward JM *et al.* Hematopoietic, angiogenic and eye defects in Meis1 mutant animals. *EMBO J* 2004; **23**: 450–459.
49 Wong P, Iwasaki M, Somervaille TC, So CW, Cleary ML. Meis1 is an essential and rate-limiting regulator of MLL leukemia stem cell potential. *Genes Dev* 2007; **21**: 2762–2774.
50 Horton SJ, Grier DG, McGonigle GJ, Thompson A, Morrow M, De Silva I *et al.* Continuous MLL-ENL expression is necessary to establish a 'Hox Code' and maintain immortalization of hematopoietic progenitor cells. *Cancer Res* 2005; **65**: 9245–9252.
51 Jin G, Yamazaki Y, Takuwa M, Takahara T, Kaneko K, Kuwata T *et al.* Trib1 and Evi1 cooperate with Hoxa and Meis1 in myeloid leukemogenesis. *Blood* 2007; **109**: 3998–4005.

Supplementary Information accompanies the paper on the Leukemia website (http://www.nature.com/leu)

Immunologically silent cancer clone transmission from mother to offspring

Takeshi Isoda[a,1], Anthony M. Ford[b,1], Daisuke Tomizawa[a], Frederik W. van Delft[b], David Gonzalez De Castro[b], Norkio Mitsuiki[a], Joannah Score[c], Tomohiko Taki[d], Tomohiro Morio[a], Masatoshi Takagi[a], Hiroh Saji[e], Mel Greaves[b,2,3], and Shuki Mizutani[a,2,3]

[a]Department of Pediatrics and Developmental Biology, Tokyo Medical and Dental University, 1-5-45 Yushima, Bunkyo-ku, Tokyo 1138519, Japan; [b]Section of Haemato-Oncology, Institute of Cancer Research, Brookes Lawley Building, 15 Cotswold Road, Sutton, Surrey SM2 5NG, United Kingdom; [c]Wessex Regional Genetics Laboratory, University of Southampton, Salisbury District Hospital, Salisbury SP2 8BJ, United Kingdom; [d]Department of Molecular Laboratory Medicine, Kyoto Prefectural University of Medicine Graduate School of Medical Science, 465 Kajii Cho, Hirokoji-agaru, Kawaramachi, Kamigyo-ku, Kyoto 6028566, Japan; and [e]Human Leukocyte Antigen Laboratory, Ebis Building, 3-4F, 82 Shimo-Tsutsumimachi, Marutamachi-kudaru, Kawabata Dori, Sakyo-ku, Kyoto 606-8396, Japan

Edited by Janet D. Rowley, University of Chicago Medical Center, Chicago, IL, and approved July 28, 2009 (received for review April 28, 2009)

Rare cases of possible materno-fetal transmission of cancer have been recorded over the past 100 years but evidence for a shared cancer clone has been very limited. We provide genetic evidence for mother to offspring transmission, in utero, of a leukemic cell clone. Maternal and infant cancer clones shared the same unique *BCR-ABL1* genomic fusion sequence, indicating a shared, single-cell origin. Microsatellite markers in the infant cancer were all of maternal origin. Additionally, the infant, maternally-derived cancer cells had a major deletion on one copy of chromosome 6p that included deletion of HLA alleles that were not inherited by the infant (i.e., foreign to the infant), suggesting a possible mechanism for immune evasion.

fetus | fusion gene | leukemia

Rare cases of melanoma or hemopoietic malignancies in infants have been recorded that may have been of maternal origin (1). Genetic evidence for a shared, materno-fetal clone of cancer cells has, however, to date, been sparse and based upon limited karotype information (1). Unambiguous attribution of transmission of a cancer clone should be achievable by genetic fingerprinting, the most striking precedent for which is canine transmissible venereal sarcoma (CTVS) in which multiple cases worldwide derive from a single clone (2). Leukemia fusion genes, generated by chromosome translocations, have patient-specific or idiosyncratic genomic sequences at the fusion breakpoints and are frequently early or initiating events (3). They therefore provide stable, specific, and sensitive clonal markers and can unambiguously identify a single-cell origin in different individuals as documented with monozygotic twins with concordant leukemia (4). We report here equivalent genetic scrutiny of a case of concordant maternal and infant ALL/lymphoma with the *BCR-ABL1* fusion gene.

Results

The Mother. The Japanese mother was 28 years old at her child's delivery. No hematological abnormalities had been identified during the pregnancy, and the birth was uncomplicated. Thirty-six days after the delivery, the mother experienced vaginal bleeding. On day 39, she developed fever, and on day 43, bleeding became uncontrollable. Blood showed leukocytosis (206,800/μL) with 97% lymphoblasts, anemia (hemoglobin level: 3.5g/dL), and thrombocytopenia (platelet count: $0.2 \times 10^4/\mu$L). Bone marrow aspiration revealed peroxidase-negative lymphoblasts (99.6% of nucleated cells), which were positive for CD10, CD19, CD20, CD34, TdT, and CD79a. Chromosomal G-banding showed 46,XX,t (9, 22)(q34;q11), and 3.2×10^5 copies/μgRNA of p190-type *BCR-ABL1* mRNA were detected by RT-PCR. She was diagnosed as having B-cell precursor Ph+ ALL (see *SI Text* for clinical treatment).

The Infant. The 11-month-old female offspring of the above mother was admitted to hospital with right cheek swelling. MRI revealed a mass in the cheek (Fig. S1*A*) and a pleural effusion of the lung. There was no lymph node swelling or organomegaly. She was born with normal delivery at 40 weeks, 5 days gestation. There was no history of prenatal abnormalities including intrauterine growth retardation, and she showed normal growth and development until admission.

Laboratory Findings on Infant Samples. Laboratory analyses of the maternal and infant samples was carried out with full ethical approval in accordance with the Declaration of Helsinki (Local ethics approval # CCR2285) and with informed consent of the family (father). Biopsy of the primary jaw tumor showed the presence of small round blue cell tumor with large nucleus/cytoplasm ratio, which diffusely proliferated with partial hyalinization of stroma. A large antibody panel was used to distinguish a sarcoma from lymphoma. LCA, CD10, CD20, CD79a, TdT, CD34, and MIC2 were positive by immunohistochemical staining, and CD3, CD5, CD56, desmin, HHF35, S100, GFAP, chromogranin, and synaptophysin were all negative. No cytogenetic analysis was performed but subsequent FISH analysis revealed positivity for the *BCR-ABL1* gene (Fig. S1*B*).

Cells (48.2%) in the pleural fluid were positive for CD10, CD19, CD34, and HLA-DR and p190-type *BCR-ABL1* chimeric mRNA was detected (9.5×10^4 copies/μgRNA) by quantitative RT-PCR (Q-PCR).

Blood count findings on the infant were as follows; WBC 10,100/μL (segment forms 22%; lymphocytes 72%; monocytes 5%; eosinophil 1%), hemoglobin level 12.5 g/dL, platelet count $38.4 \times 10^4/\mu$L. No blast cells were detected in the cerebrospinal fluid, and there was no morphological evidence of tumor infiltration in bone marrow. Bone marrow aspirates were negative for *BCR-ABL1* chimeric mRNA by Q-PCR. The patient's neoplastic cells had the same immunophenotype and abnormal genotype (*BCR-ABL1* fusion) as her mother's ALL but, in light of the presentation features, she was diagnosed as having B-cell precursor lymphoblastic lymphoma stage III by the St. Jude Staging System (see *SI Text* for clinical treatment of infant).

Author contributions: M.G. and S.M. designed research; A.M.F., D.T., F.W.v.D., D.G.D.C., N.M., J.S., T.T., T.M., M.T., and H.S. performed research; T.I. contributed new reagents/analytic tools; M.G. and S.M. analyzed data; and M.G. and S.M. wrote the paper.

The authors declare no conflict of interest.

This article is a PNAS Direct Submission.

[1]T.I. and A.M.F. contributed equally to this work.

[2]M.G. and S.M. contributed equally to this work.

[3]To whom correspondence may be addressed. E-mail: mel.greaves@icr.ac.uk or skkm12@gmail.com.

This article contains supporting information online at www.pnas.org/cgi/content/full/0904658106/DCSupplemental.